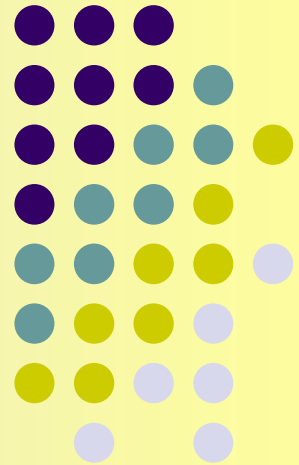


Exploring the possibility of studying the Drell-Yang process in the SPD (NICA) experiment.

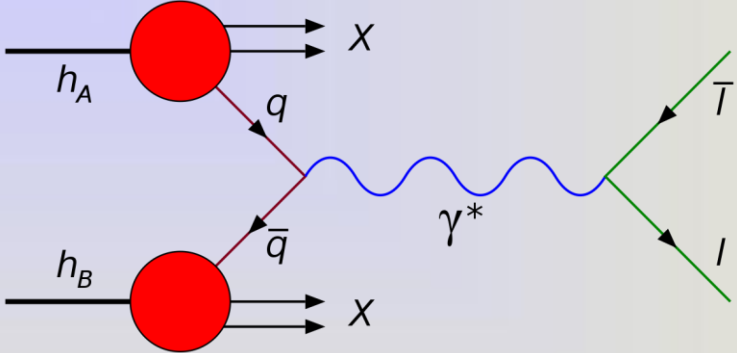
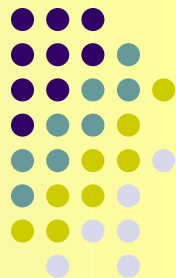


A.N.Skachkova
(JINR, Dubna)

**The XV-th International
School-Conference
"The Actual Problems of
Microworld Physics"**



Minsk, Belarus, 27 August – 3 September, 2023

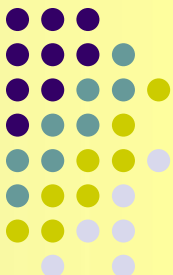


Процессы Дрелл-Яна представляют собой столкновения адронов при высоких энергиях, рождающих при взаимодействии кварка и антiquарка нейтральный калибровочный бозон — виртуальный фотон или слабый Z0 бозон, который затем распадается на пару противоположно заряженных лептонов

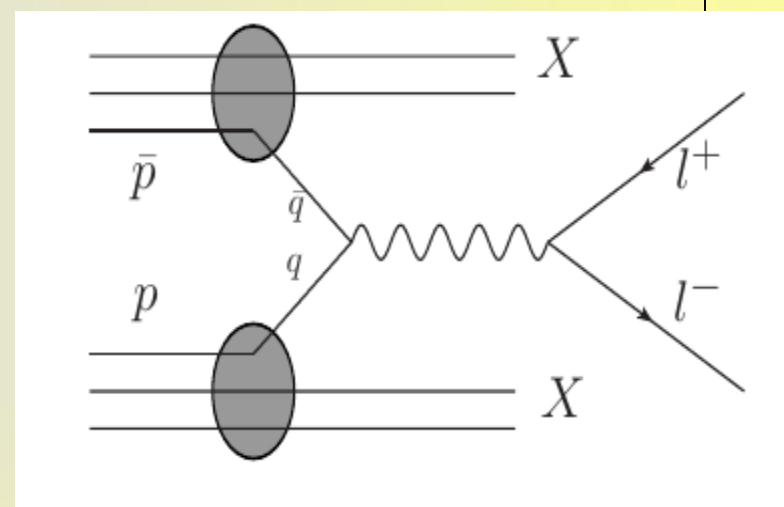
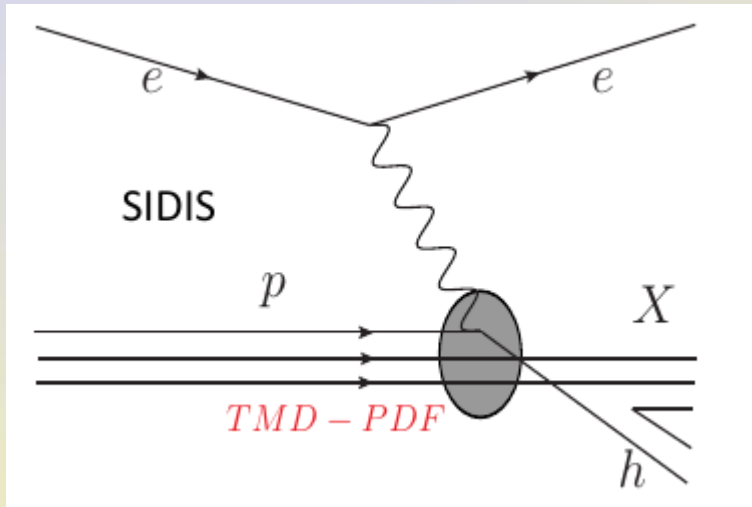
Они являются уникальными процессами для исследования спиновых эффектов в адронных взаимодействиях, позволяют получить доступ к **партональным распределениям** (*описывающим распределения кварков и глюонов в адронах (ядрах) по двум переменным: x (доля продольного момента k адрона, переносимого активным partonом) и pT (поперечного импульса активного partона))* и извлечь новую информацию о структуре ядерной материи и элементарных частиц.

Прецизионное извлечение партональных распределений из одних экспериментальных данных позволяет использовать их для предсказаний в других физических процессах.

Экспериментальные исследования процессов Дрелл-Яна позволяют непосредственно измерить различные спиновые асимметрии в столкновениях неполяризованных, поперечно- и продольно-поляризованных адронов.



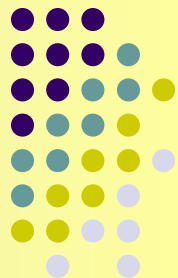
Реакции Дрелла-Яна являются важным дополнением к другим реакциям (таким как, например, полуинклюзивные реакции глубоконеупругого рассеяния (SIDIS)).



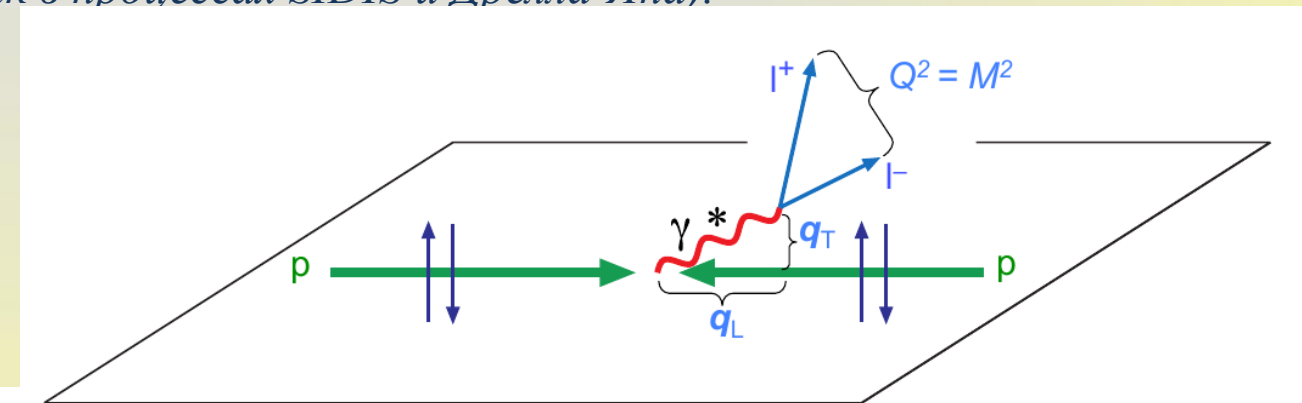
TMD-PDF связаны с функциями фрагментации

Почему Drell-Yan? - Прямой доступ к TMD-PDFs

По отношению к DIS (инклюзивному или полу-инклюзивному) путем вращения Фейнмановской диаграммы, Drell-Yan является s-канальным процессом, а SIDIS - t-канальным.



Анализ измеренных спиновых характеристик позволяет извлечь информацию о партонных импульсных распределениях TMD (относительно поперечного и продольного импульса активного партона) и PDF (относительно продольного импульса активного партона), являющихся универсальными непертурбативными функциями (описывающие эффекты на больших расстояниях / или при малых значениях импульсов), не зависящими от типа физического процесса характеристиками (за исключением T -нечетных TMD (T -odd TMD Боера-Малдерса и Сиверса), меняющим знак в процессы SIDIS и Дрелла-Яна).

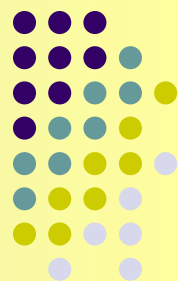


$$d\sigma^{D-Y} = \sum f_q(x_1, \mathbf{k}_{\perp 1}; Q^2) \otimes f_{\bar{q}}(x_2, \mathbf{k}_{\perp 2}; Q^2) d\hat{\sigma}^{q\bar{q} \rightarrow \ell^+ \ell^-}$$

Для извлечения PDF распределений наиболее подходит условия когда когда M_{inv} ($=Q$ -переданный 4-х импульс) и РТ одного порядка. Для извлечения информации о TMD распределениях идеален масштаб M_{inv} ($=Q$) \gg РТ лептонной пары \sim поперечного импульса夸ков и глюонов kT внутри сталкивающихся адронов.

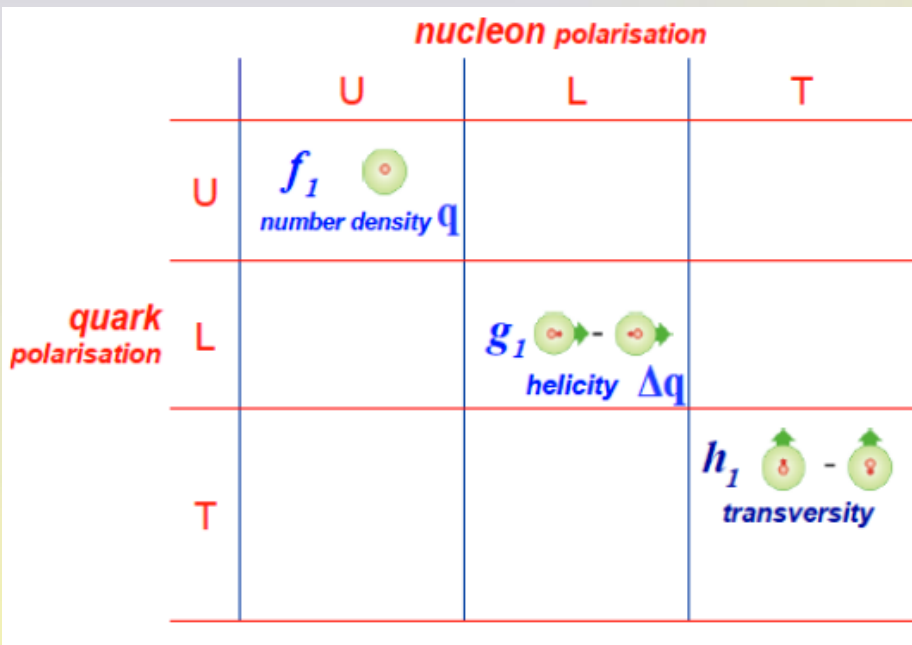
Партонные распределения есть матричные элементы операторов, построенных в терминах кварковых и глюонных полей, и усредненных по адронным состояниям (состояния вакуума).

Parton Distribution Functions



A number of PDFs depends on the order of the QCD approximations.

At leading order (LO, twist-2) 3 collinear (integrated over kt) PDFs are needed for a full description of the nucleon structure:



The PDFs f_1 and g_1 are measured rather well. The PDF h_1 (x, Q^2) is poorly studied. *It was historically introduced right for DY process.*

- **Density f_1 (x, Q^2)** — distribution of the parton Number/ probability to find quarks within the non-polarized (U) nucleon carrying a fraction x of the nucleon momentum

$$f_1 = \text{○}$$

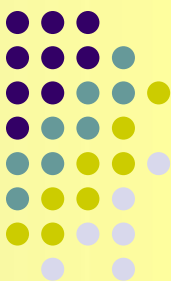
- **Helicity (chirality) g_1 (x, Q^2) $\equiv g_{1L}$ (x, Q^2)** distribution of longitudinal polarization of quarks in longitudinally polarized (L) nucleon/ the difference in probabilities to find quarks in a longitudinally polarized nucleon with their spin aligned or anti- aligned to the spin of the nucleon

$$g_{1L} = \text{○} \rightarrow - \text{○} \rightarrow$$

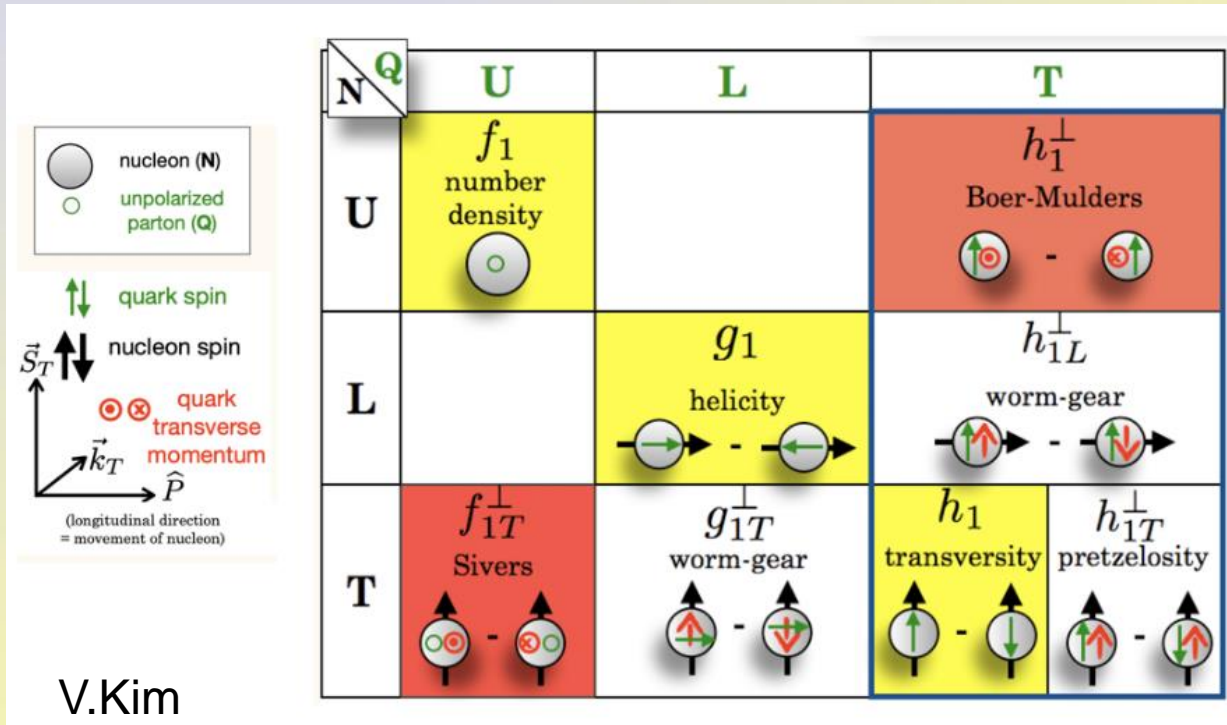
- **Transversity h_1 (x, Q^2)** - distribution of transverse polarization of quarks in transversely polarized (T) nucleon

$$h_{1T} = \text{○} \uparrow - \text{○} \downarrow$$

The structure of the proton: TMD PDF



Taking into account the quark **intrinsic transverse momentum k_T** , at leading order 8 TMD (**5 additional**) PDFs are needed for a full description of the nucleon structure, which are *functions of 3 variables* (x, kT, Q^2). They are vanishes when integrating over kT .

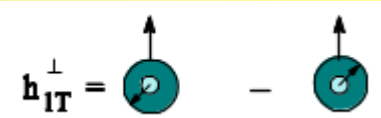
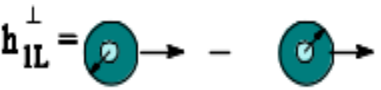
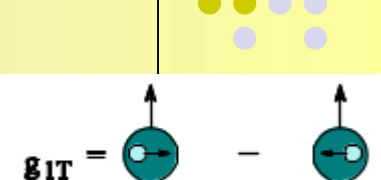
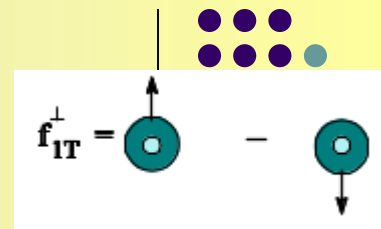


Leading twist TMD distribution functions. The **U,L,T** correspond to **unpolarized**, **longitudinally polarized** and **transversely polarized** nucleons (columns) and quarks (rows).

At the sub-leading twist (twist-3), there are still 16 TMD PDFs containing the information on the nucleon structure. *They have no definite physics interpretation yet.*

Since TMD distributions are nonperturbative functions, they **cannot be calculated within the framework of QCD**. Therefore, the main model-independent tool for studying TMD is **the analysis of spin effects in SIDIS and Drell-Yang processes**.

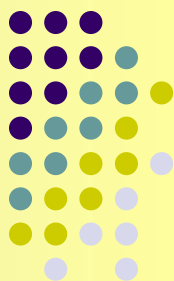
- **f_{1T}^\perp (Sivers)** - represents the distribution over the transverse momentum of non-polarized quarks in a transversely polarized nucleon (transverse spin);
- **g_{1T}^\perp (Worm-gear-T)** - correlation between the transverse spin and the longitudinal quark polarization;
- **h_1^\perp (Boer-Mulders)** - distribution over the transverse momentum of transversely polarized quarks in the non-polarized nucleon ;
- **h_{1L}^\perp (Worm-gear-L)** - correlation between the longitudinal polarization of the nucleon (longitudinal spin) and the transverse momentum of quarks;
- **h_{1T}^\perp (Pretzelosity)** - distribution over the transverse momentum of transversely polarized quarks in the transversely polarized nucleon.



It is very important to measure Worm-gear-T, L and Pretzelosity which are still not measured or measured with large uncertainties.

The last one would give new information (at least within some models) on the possible role of constituent's orbital momenta in the resolution of the nucleon spin crisis.

The PDFs studies via asymmetry of the DY pairs production cross sections

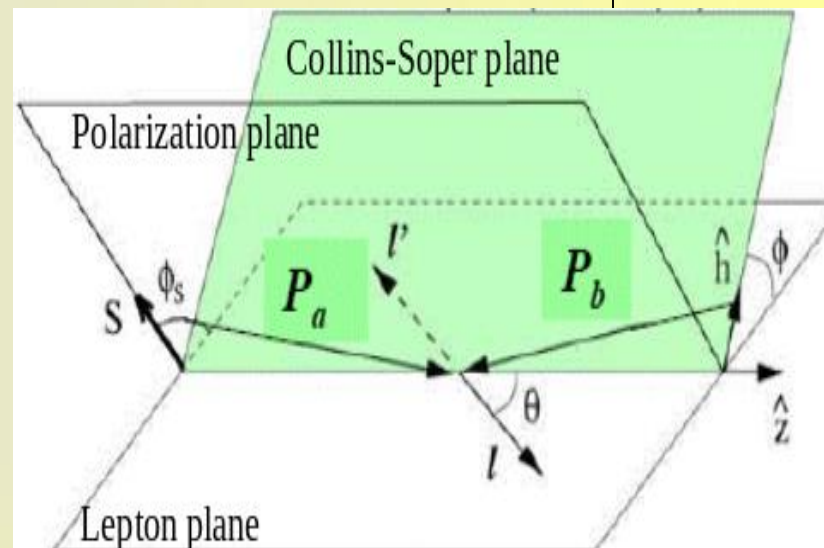


The cross section of the DY pair's production **cannot be measured directly** because there is **no single beam containing particles with the U, L and T polarization**.

To **measure SF's** one can use the following procedure:

1-st - to integrate differential cross section over the azimuthal **angle ϕ** between the Lepton and Hadron planes in the Collins-Soper reference frame,

2-nd - following the SIDIS practice, to measure azimuthal asymmetries of the DY pairs production cross sections.



The **azimuthal asymmetries** can be **calculated as ratios of cross sections differences** to the **sum** of the integrated over ϕ **cross sections** σ_{int} :

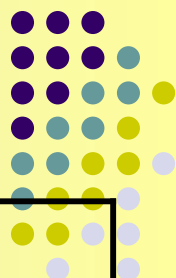
- The **numerator** of the ratio is calculated as a **difference** of the DY pair's production **cross sections** in the collision of hadrons h_a and h_b with **different polarizations**.
- The **denominator** of the ratio is calculated as a **sum of** σ_{int} 's calculated for the **same hadron polarizations** and same x_a, x_b regions **as in numerator**.

Previous Drell-Yan experiments

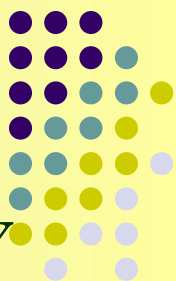


Experiment	Interaction	Reaction	Energy	
CERN-NA3	pN(Pt)	p Nucleus --> mu+ mu- X	Plab	= 400 GeV
CERN-NA10	pi-N(W)	pi- Nucleus --> mu+ mu- X	Plab	= 194, 286 GeV
CERN-NA58 (COMPASS)	pi-p	pi p → mu+ mu- X	Plab	= 190 GeV
CERN-WA11	pi-N(Be)	pi- Nucleus --> mu+ mu- X	Plab	= 150/175 GeV
CERN-WA39	pi+N(W) pi-N(W)	pi+ Nucleus --> mu+ mu- X, pi- Nucleus --> mu+ mu- X	Plab	= 39.5 GeV
CERN-R108	pp	p p --> e+ e- X	Plab(Ecm)	= 62.4 GeV
CERN-R209	pp	p p --> mu+ mu- X	Plab (sqrt(s))	= 44, 62 GeV
CERN-R808	pp	p p --> e+ e- X	Plab (sqrt(s))	= 53, 63 GeV
CERN-UA2	pbar p	pbar p --> mu+ mu- X	Plab	= 630 GeV
Fermilab-E288	pN(Pt)	p Nucleus --> mu+ mu- X	Plab	= 200/300/400 GeV
Fermilab-E325	pN(Cu)	p Nucleus --> mu+ mu- X	Plab	= 200,300,400 GeV
Fermilab-E326	pi-N(W)	pi- Nucleus --> mu+ mu- X	Plab	= 225 GeV
Fermilab-E439	pN(Cu)	p Nucleus --> mu+ mu- X	Plab	= 400 GeV
Fermilab-E444	pN(C, Cu, W)	p Nucleus --> mu+ mu- X, pi+ Nucleus --> mu+ mu- X, pi- Nucleus --> mu+ mu- X	Plab	= 225 GeV
Fermilab-E537	Pbar N(W), pi- N(W)	pbar p --> e+ e- X, pbar N --> mu+ mu- X, pi- Nucleus --> mu+ mu- X	Plab	= 125 GeV
Fermilab-E605	pN(Cu)	p Nucleus --> mu+ mu- X	Plab	= 800 GeV
Fermilab-E615	pi- N(W)	pi- Nucleus --> mu+ mu- X	Plab	= 252 GeV
Fermilab-E740(D0)	pbar p	pbar p --> e+ e- X	Ecms (sqrt(s))	= 1800 GeV
Fermilab-E741(CDF)	pbar p	pbar p --> mu+ mu- X , pbar p --> e+ e- X	Ecms (sqrt(s))	= 1800 GeV
Fermilab-E772	pp	p p --> mu+ mu- X	Plab	= 800 GeV
Fermilab-E866(NUSEA)	pp	p p --> mu+ mu- X	Plab	= 800 GeV

Experiments studying nucleon spin structure



<i>experiment</i>	CERN, COMPASS-II	FAIR, PANDA	FNAL, E-906	RHIC, STAR	RHIC- PHENIX	NICA, SPD
<i>mode</i>	Fixed Target	Fixed T.	Fixed T.	collider	collider	collider
<i>Beam/target</i>	π^- , p	anti-p, p	π^- , p	pp	pp	pp, pd, dd
<i>Polarization:</i> b/t	0; 0.8	0; 0	0; 0	0.5	0.5	0.9
<i>Luminosity</i>	$2 \cdot 10^{33}$	$2 \cdot 10^{32}$	$3.5 \cdot 10^{35}$	$5 \cdot 10^{32}$	$5 \cdot 10^{32}$	10^{32}
\sqrt{s} , GeV	19	<5.5	16	200, 500	200, 500	10 - 26
$x_{1(\text{beam})}$ range	0.1-0.9	0.1-0.8	0.1-0.5	0.03-1.0	0.03-1.0	0.1-0.8
q_T , GeV	0.5 -4.0	0.5 -1.5	0.5 -3.0	1.0 -10.0	1.0 -10.0	0.5 -6.0
<i>Lepton pairs,</i>	$\mu-\mu^+$	$\mu-\mu^+$	$\mu-\mu^+$	$\mu-\mu^+$	$\mu-\mu^+$	$\mu-\mu^+, e+e^-$
<i>Data taking</i>	2015	>2025	2013	>2016	>2016	>2020
<i>Transversity</i>	NO	NO (?)	NO	YES	YES	YES
<i>Boer-Mulders</i>	YES	YES	YES	YES	YES	YES
<i>Sivers</i>	YES	YES (?)	YES	YES	YES	YES
<i>Pretzelosity</i>	NO	NO	NO	NO	YES	YES
<i>Worm Gear</i>	NO	NO	NO	NO	NO	YES

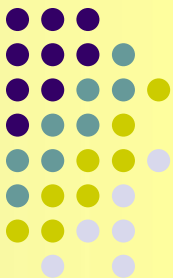


The tests at the SPD would have a number of advantages for DY measurements related to the nucleon structure studies:

- Running with **pp, pd and dd** beams,
- Scan of the effects over a *range of beam energies*,
- Running with **non-polarized, transverse and longitudinally polarized** beams and their combinations.

The above advantages would permit, for the first time, to perform comprehensive studies of **all leading twist PDFs** of the nucleon in a **single experiment** with minimal systematic errors.

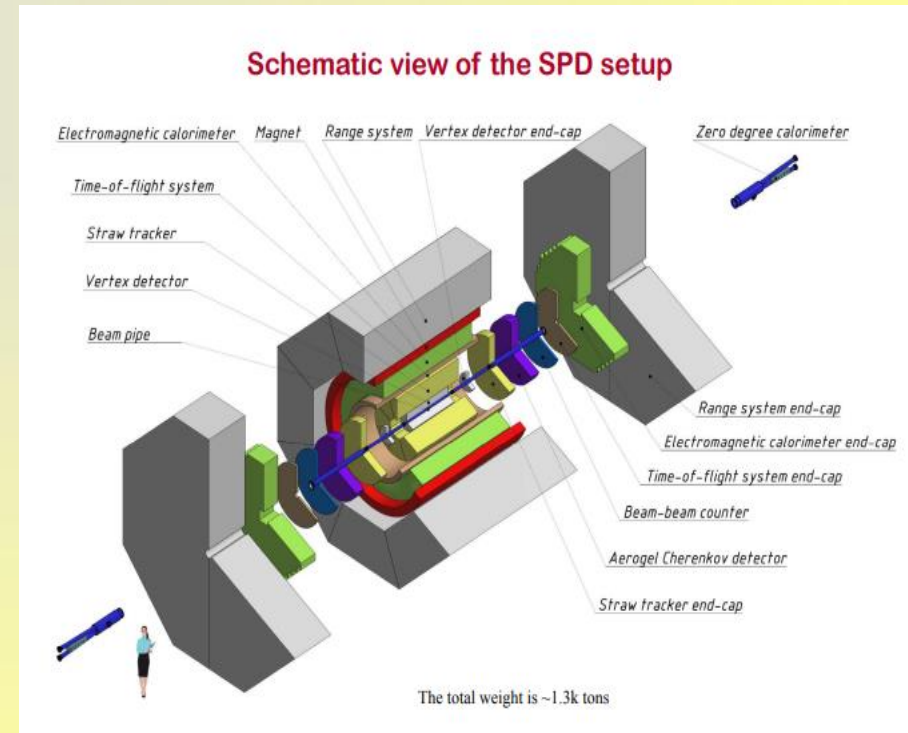
SPD — Spin Physics Detector

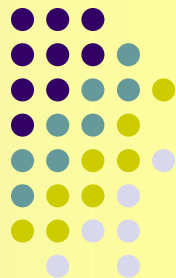


Beam energies:

$p\uparrow-p\uparrow(\sqrt{s_{pp}}) = 12 \div 27 \text{ GeV}$ ($5 \div 12.6 \text{ GeV}$ of proton kinetic energy),
 $d\uparrow-d\uparrow(\sqrt{s_{NN}}) = 4 \div 13.5 \text{ GeV}$ ($2 \div 5.9 \text{ GeV/u}$ of ion kinetic energy),
 $p\uparrow-d\uparrow(\sqrt{s_{NN}}) \leq 19 \text{ GeV}$

- Luminosity up to $1 \cdot 10^{32} \text{ cm}^{-2}\text{s}^{-1}$ (p-p)
- $0.25 \cdot 10^{32} \text{ cm}^{-2}\text{s}^{-1}$ (d-d)
- Universal 4π detector with advanced tracking and particle identification capabilities based on modern technologies.
- Capability to detect events with high collision rate (up to 4MHz)
- Tracking : $\sim <100 \mu\text{m}$ vertex resolution
- Photon detection with the energy resolution $\sim 5\%/\text{VE}$
- Transverse momentum resolution $\sigma_{\text{pT}} \approx 2\%$

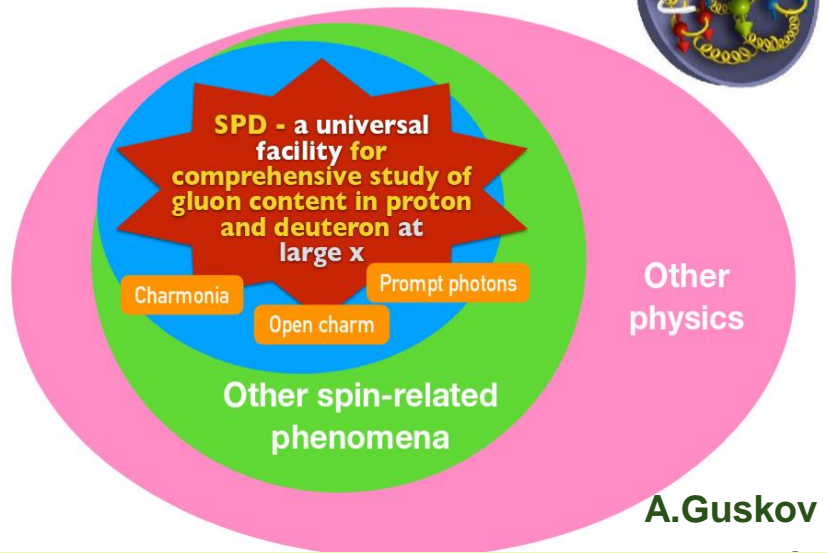




SPD Physics Program

The Spin Physics Detector (SPD) project aims to investigate the nucleon spin structure and polarization phenomena in polarized p-p and d-d collisions.

CONCEPT OF THE SPD PHYSICS PROGRAM

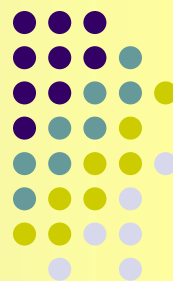


«Possible studies at the first stage of the NICA collider operation with polarized and unpolarized proton and deuteron beams» arXiv:2102.08477, 2021

«On the physics potential to study the gluon content of proton and deuteron at NICA SPD» arXiv:2011.15005, 2021

The plans to study Drell-Yan (DY) at SPD initially were the first in the list of physics proposal at SPD facility

«Spin Physics Experiments at NICA-SPD with polarized proton and deuteron beams». Lol arXiv:1408.3959, 2014



V.A. Matveev, R.M. Muradian, A.N. Tavkhelidze (MMT)

(V.A. Matveev, R.M. Muradian, A.N Tavkhelidze, JINR-P2-4543, JINR, Dubna, 1969; SLAC-TRANS-0098)

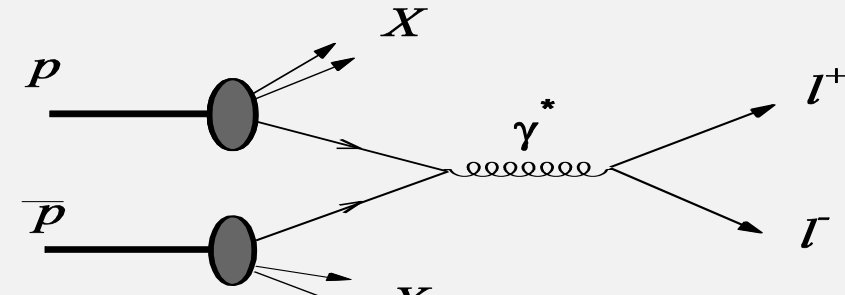
process, called also as Drell-Yan

(S.D. Drell, T.M. Yan, SLAC-PUB-0755, Jun 1970, 12p.; Phys.Rev.Lett. 25(1970)316-320, 1970)

The dominant mechanism
of the $\ell^+ \ell^-$ production is
the perturbative QED/QCD
partonic $2 \rightarrow 2$ process

$$\bar{q}q \rightarrow \gamma^*/Z^* \rightarrow \ell^+ \ell^-$$

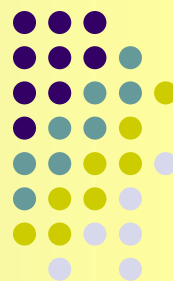
$$\sigma = 9.6 * 10^3 \text{ pb}$$



PYTHIA 6.4 simulation for the $E_{(p-p) \text{ cms}} = 27 \text{ GeV}$

For the Luminosity $L = 1 \times 10^{32} \text{ cm}^{-2}\text{s}^{-1}$ with assumption of 10^7 sec/year of beam operation we expect up to 9.5×10^6 Drell-Yan events/year (without any cuts) & $\sim 79,700$ Drell-Yan events/year for $M_{\text{inv}}(\mu^+ \mu^-) > 4 \text{ GeV}$ (and first 2 cuts)

Main backgrounds



Main contribution to backgrounds for $\bar{q} q \rightarrow \gamma^* \rightarrow \mu^+ \mu^-$ process comes from two sources:
QCD (+charmonium) and Minimum-bias events

Initial conditions for simulation (both signal and BKG) are:
 ISR, FSR, MPI – ON ; Lund fragmentation

We allow particles decay (and produce muons) in the volume before the Muon (Range) System :

cylindrical radius $R = 2400$ mm / size from the centre along Z axis $L = 4000$ mm
 and search for muons in the angle region $3^\circ < \Theta < 177^\circ$

Contribution from b-quarks (subprocesses 81, 82, 461- 479) is negligible.

Total cross-section is 0.34×10^{-6} mb. Initial S/B ≈ 27 .

Contribution from charmonia (subprocesses 86, 87-89, 104-105, 106, 421-439)
is less than from QCD and Mini-bias, but significant.

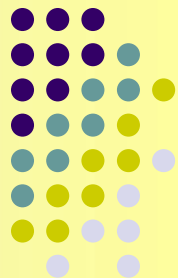
Their cross-section is 8.6×10^{-4} mb. Initial S/B = 1.0×10^{-2} .

Contribution from Charm production (subprocesses 81. $q + q\bar{q} \rightarrow c c\bar{q}\bar{q}$
 82. $q + g \rightarrow c c\bar{q}\bar{q}$)

Total cross-section is 1.9×10^{-3} mb. Initial S/B $\approx 5.2 \times 10^{-3}$

{Easy to suppress}

Main backgrounds



Now they are included in the **total list of QCD events** modeling
(subprocesses 10-14, 28-29, 53, 68)

The main contributions come from the following partonic subprocesses:

$q + g \rightarrow q + g$ (gives 43.5% of QCD events with the $\sigma = 92.7$ mb);

$g + g \rightarrow g + g$ (gives 46.7% of QCD events with the $\sigma = 99.5$ mb);

$q + q' \rightarrow q + q'$ (gives 9.2% of QCD events with the $\sigma = 19.7$ mb);

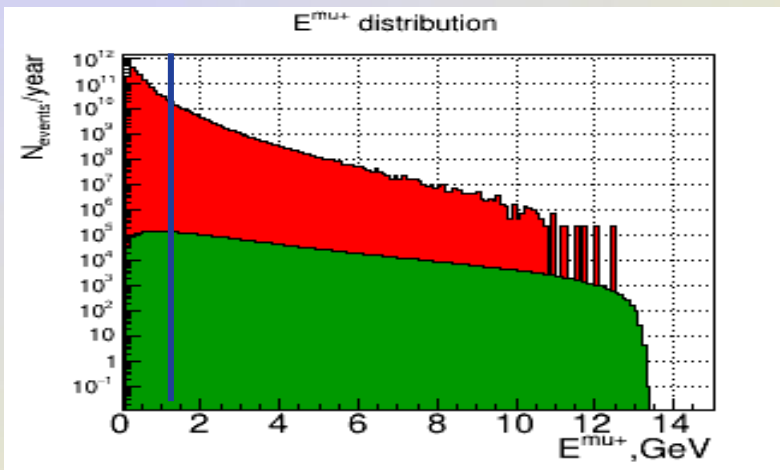
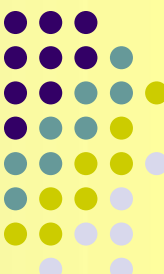
For QCD background $\sigma = 212.9$ mb, $S/B \simeq 4.6 \times 10^{-8}$
(one order stronger than Mini-bias!)

Minimum-Bias processes

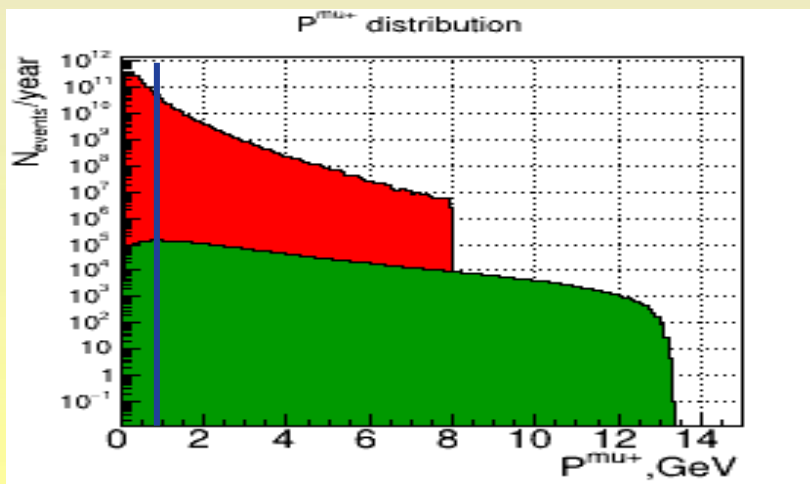
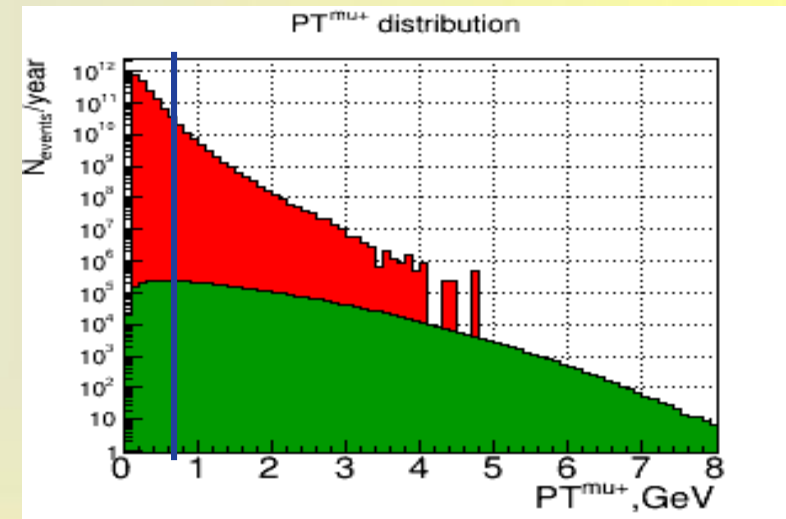
- 95. **Low - PT scattering** (~65% of MB events with the $\sigma = 14.0$ mb);
- 92-93. **Single diffractive** (24.8% of MB events with the $\sigma = 7.35$ mb);
- 94. **Double diffractive** (7.2% of MB events with the $\sigma = 2.12$ mb);

$\sigma = 23.7$ mb. **$S/B \simeq 4.2 \times 10^{-7}$**

First cuts - on E(P) and PT



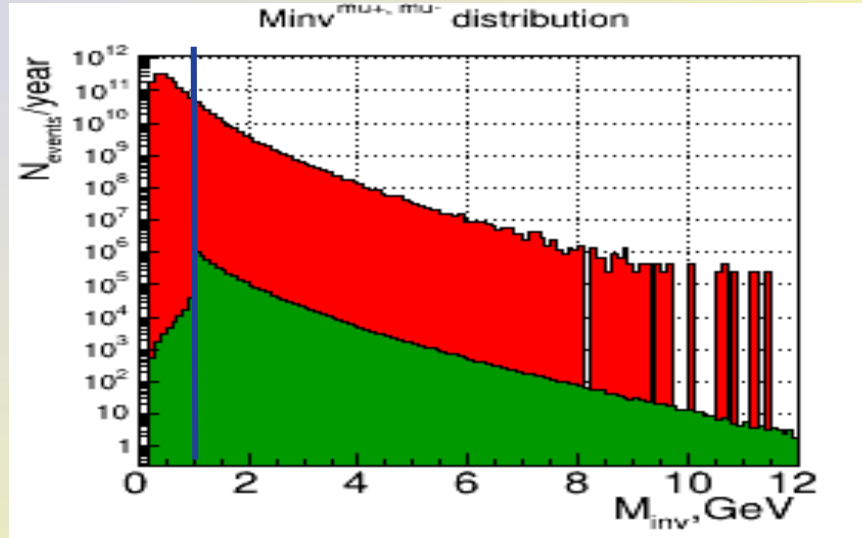
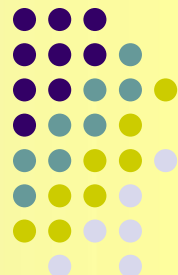
Effective cut off on E(P) only in the region
E^μ _{bkg} < 1.5 GeV (example E^μ _{bkg} = 1.0 GeV)
 where is the maximum gradient in E^μ _{bkg} distribution



The most effective cuts off are in the region
PT^μ _{bkg} < 1.5 GeV
 (for example PT^μ _{bkg} = 0.6 GeV)

Invariant mass cut

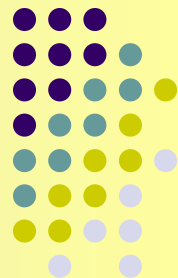
(picture corresponds to minimum-bias backgrounds)



The most effective cut is in the region **~ 1 GeV**.

Further increase of Minv cut has no sense for Minimum-bias background events (it leads to significant loss of signal events without real improvement of S/B ratio) except backgrounds in the regions of J/ Ψ and other resonances production.

Efficiency of $M_{inv} (\mu^+, \mu^-)$ cut



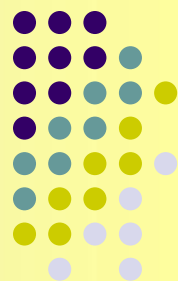
Together with the cut on $E(P)^{\mu} > 1$ GeV, $PT^{\mu} > 0.6$ GeV
and opposite sign leptons

$$Cut\ efficiency = Nev(cutN) / Nev(init)$$

Minv cut	Rest of BKG	Cut efficiency for BKG	Rest of SIG	Rest of SIG events/year	Cut efficiency for SIG	S/B
$M_{inv}^{\mu\mu} > 1.0$ GeV	1.70×10^{-2} %	1.36	40.5 %	3 869 571	1.02	1.0×10^{-4} %
$M_{inv}^{\mu\mu} > 1.5$ GeV	1.35×10^{-2} %	1.69	16.7 %	1 595 601	2.97	6.3×10^{-5} %
$M_{inv}^{\mu\mu} > 2.0$ GeV	9.57×10^{-3} %	2.41	8.3 %	793 023	7.28	4.4×10^{-5} %
$M_{inv}^{\mu\mu} > 2.5$ GeV	6.05×10^{-3} %	3.80	4.5 %	429 952	15.9	3.8×10^{-5} %
$M_{inv}^{\mu\mu} > 3.0$ GeV	3.70×10^{-3} %	6.22	2.5 %	238 862	32.0	3.4×10^{-5} %
$M_{inv}^{\mu\mu} > 3.5$ GeV	2.24×10^{-3} %	10.3	1.4 %	133 762	60.7	3.2×10^{-5} %
$M_{inv}^{\mu\mu} > 4.0$ GeV	1.38×10^{-3} %	16.7	0.8 %	76 435	110.1	2.9×10^{-5} %
$M_{inv}^{\mu\mu} > 4.5$ GeV	8.49×10^{-4} %	27.1	0.5 %	47 772	192.2	3.0×10^{-5} %
$M_{inv}^{\mu\mu} > 5.0$ GeV	5.28×10^{-4} %	43.7	0.3 %	28 663	328.0	2.9×10^{-5} %

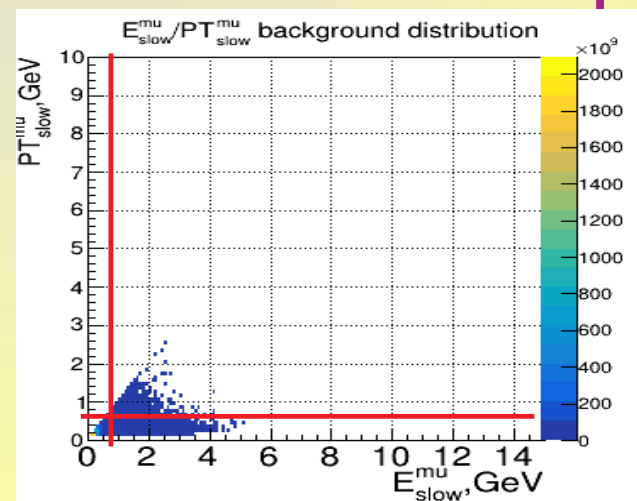
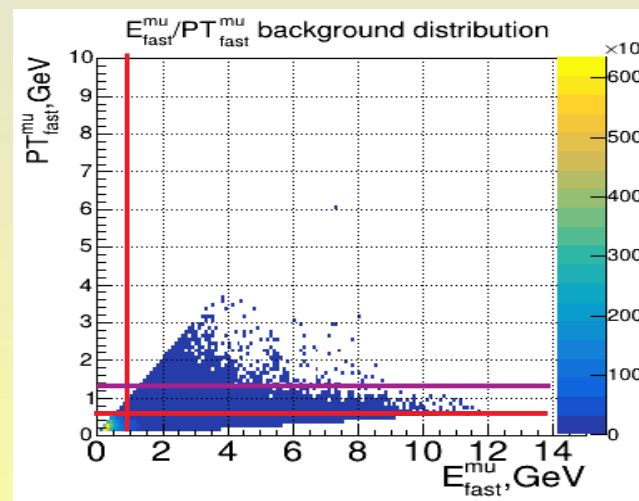
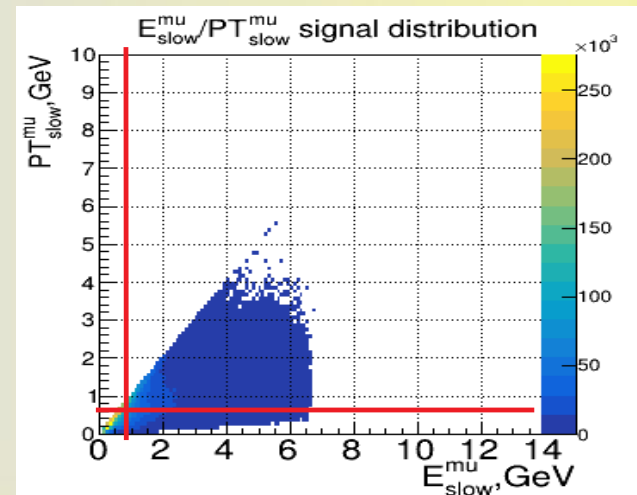
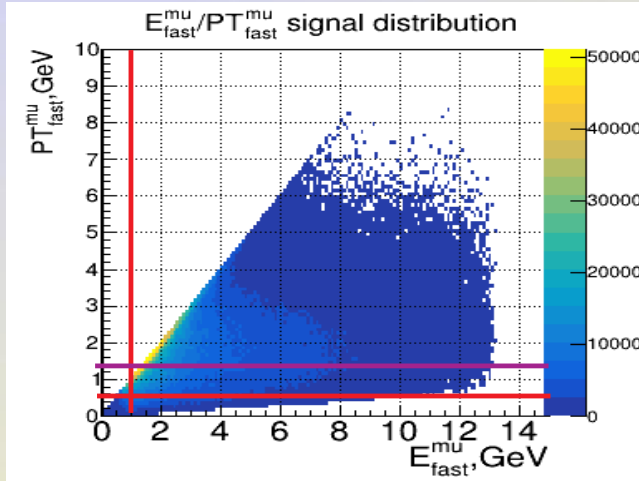
Minv cut doesn't influence much on S/B ratio. But at $M_{inv}^{\mu\mu} > 4.0$ GeV we have **too small number of events/year**.

E^μ/PT^μ correlations for muons with max(fast) / min(slow) E^μ in the pair



S
I
G

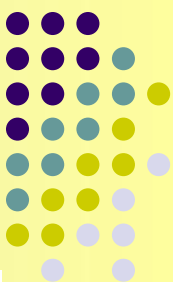
B
K
G



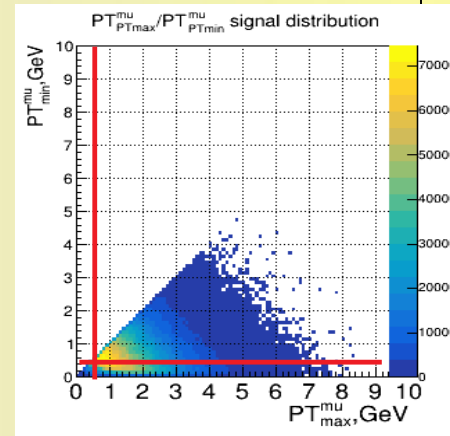
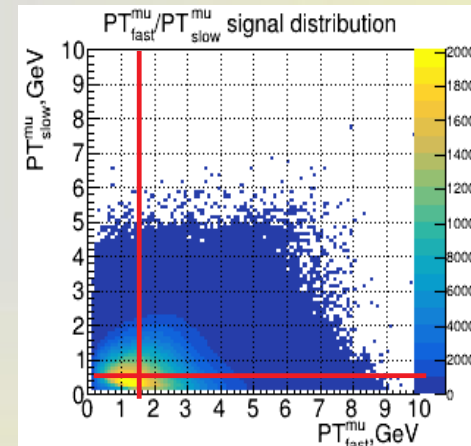
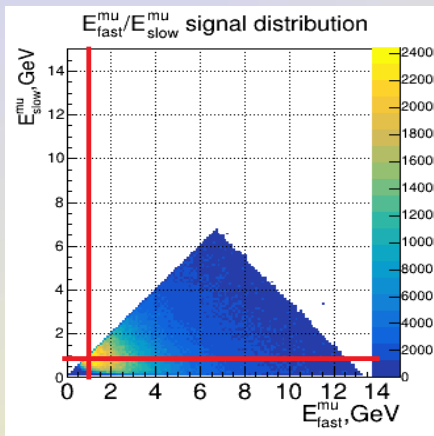
$PT^\mu_{\text{fast}} > 1.5 \text{ GeV}$

Cut on $PT^\mu > 0.6 \text{ GeV}$ and $E^\mu > 1.0 \text{ GeV}$

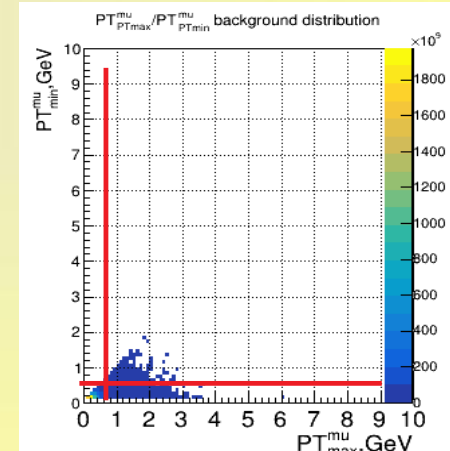
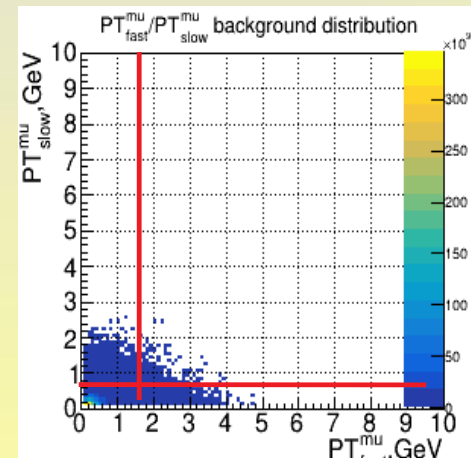
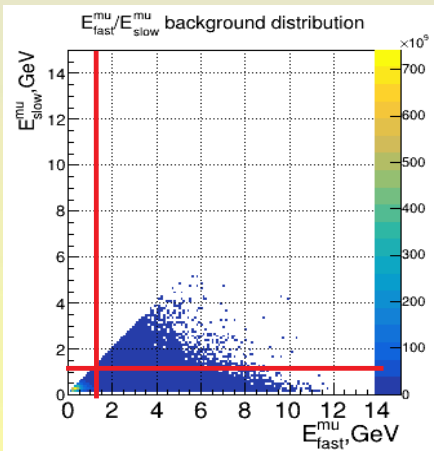
$E^{\mu}_{\text{max(fast)}}/E^{\mu}_{\text{min(slow)}}, \text{PT}^{\mu}_{\text{fast}}/\text{PT}^{\mu}_{\text{slow}},$ $\text{PT}^{\mu}_{\text{max}}/\text{PT}^{\mu}_{\text{min}}$ distributions



S
-
I
G



B
K
G

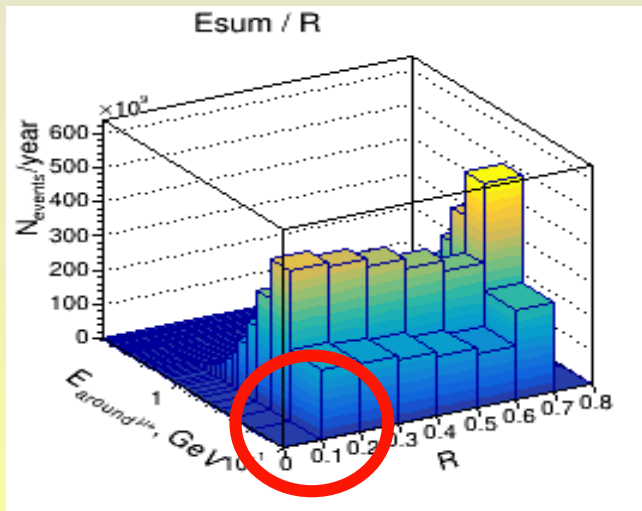
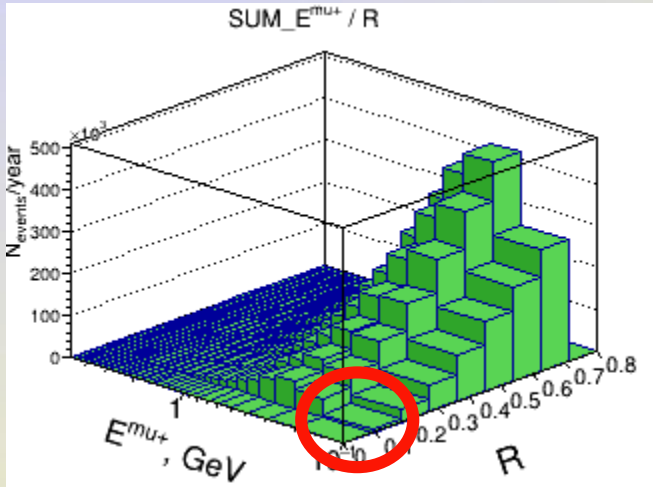


$E^{\mu} > 1.0 \text{ GeV}$

$\text{PT}^{\mu}_{\text{fast}} > 1.5 \text{ GeV}$

$\text{PT}^{\mu} > 0.6 \text{ GeV}$

Lepton (μ) isolation criteria



The plots show the distributions over **summarized energy** of the final state charged particles in the cones of radius $R_{\text{isolation}} = \sqrt{\Delta\eta^2 + \Delta\varphi^2}$ respect to the (η — pseudorapidity, φ — azimuthal angle)

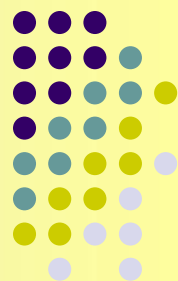
upper plot **signal events**

bottom plot **Mini-bias background**

Isolation criteria ($R_{\text{isolation}} = 0.2$)
E_{sum} (of particles) < 0.5 GeV

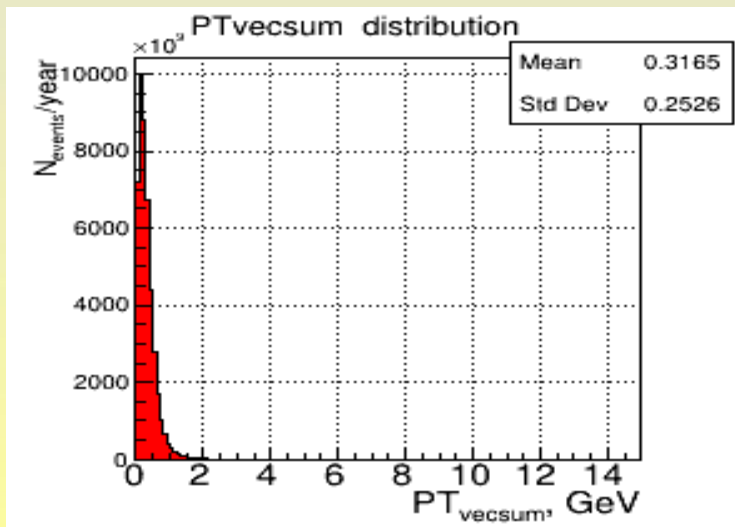
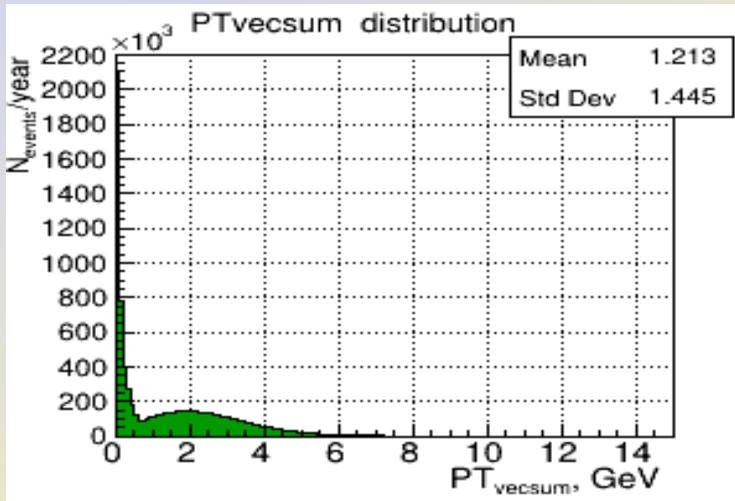
allows to separate most part of Mini-bias & QCD bkg muons
with additional loss of **0.7%** of signal events
after applied cuts discussed above

Cut on $\text{PT}_{\text{vecsum}}$ - vector sum of all particles transverse momenta in event

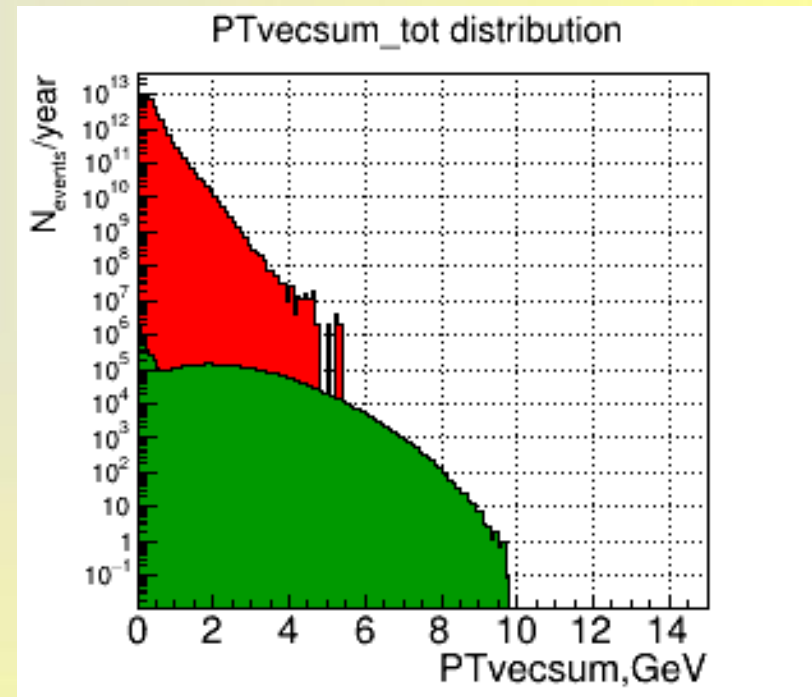


S
I
G

B
K
G

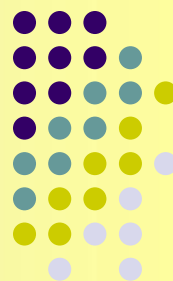


Sig & BKG
in log scale

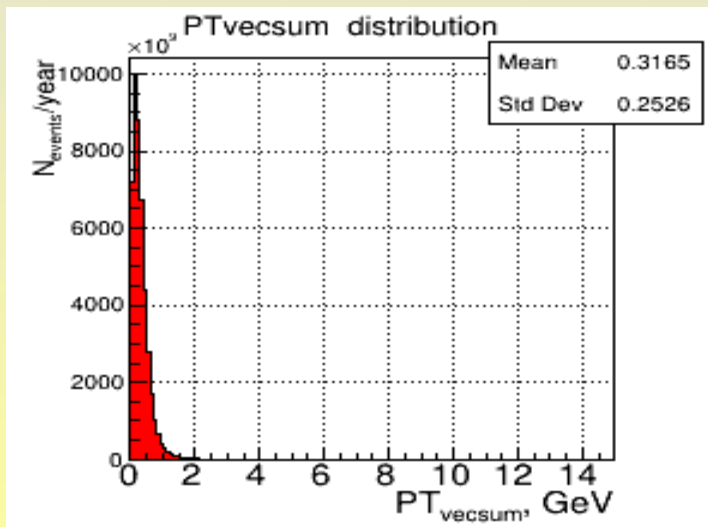
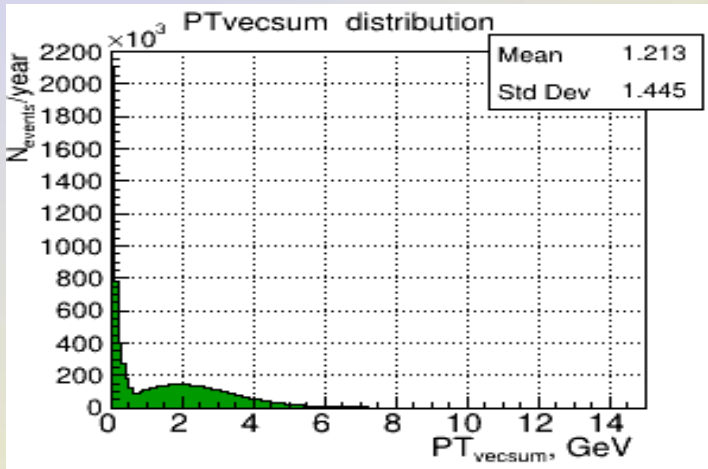


$\text{PT}_{\text{vecsum}} < 0.2 \text{ GeV}$
BKG suppression factor (Eff) = 4

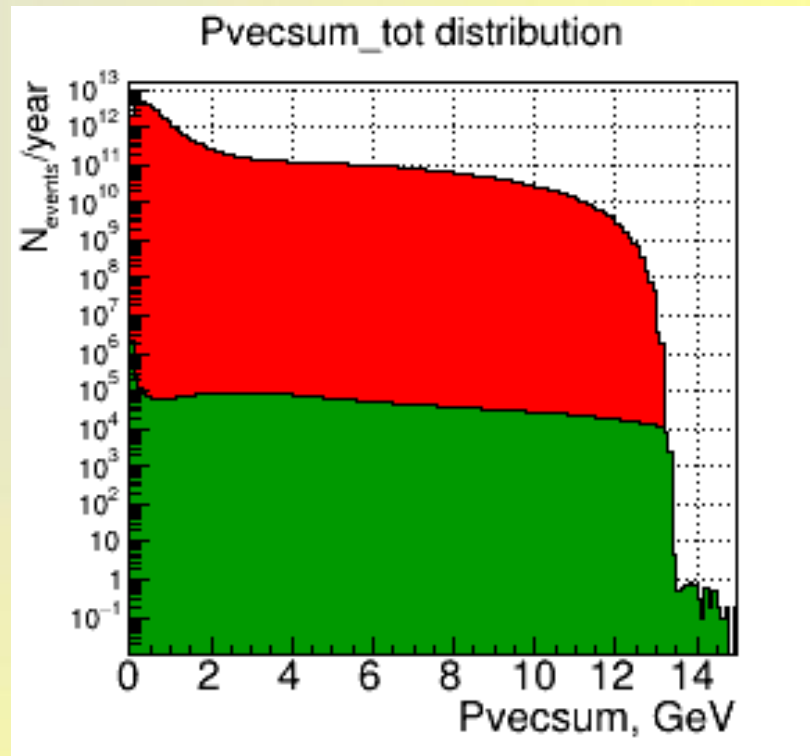
Analogous cut on P_{vecsum} - vector sum of all particles momenta in event



S
I
G

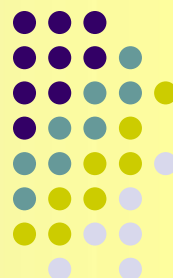


Sig & BKG
in log scale

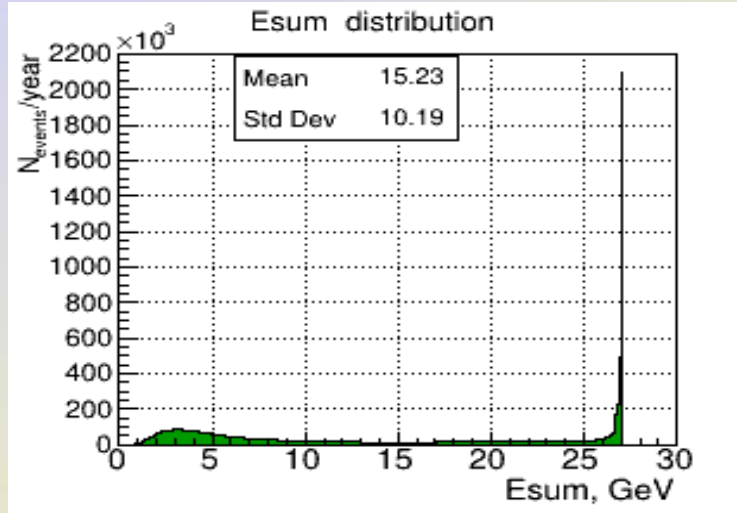


$P_{\text{vecsum}} < 0.2 \text{ GeV}$
BKG suppression factor (Eff)= 18 - 19

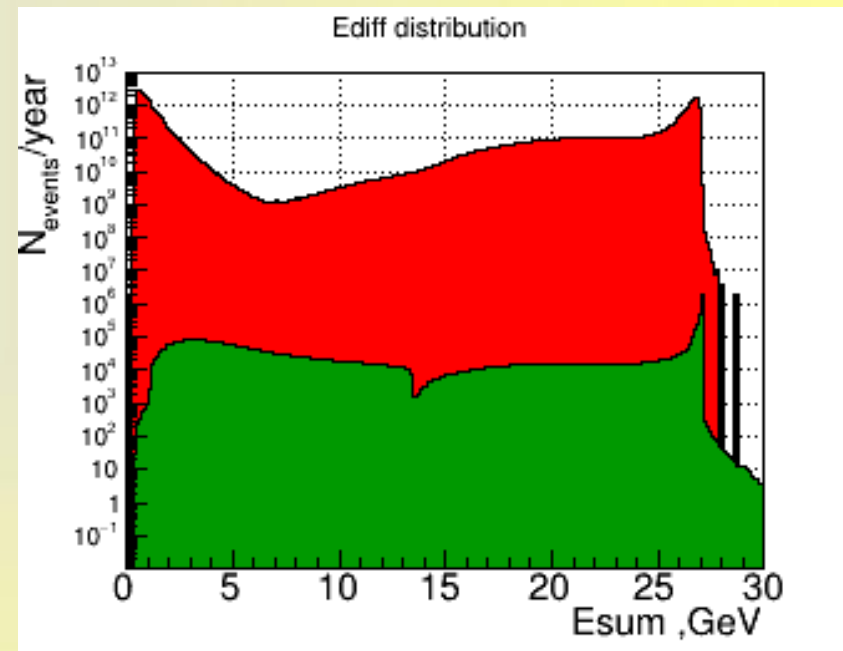
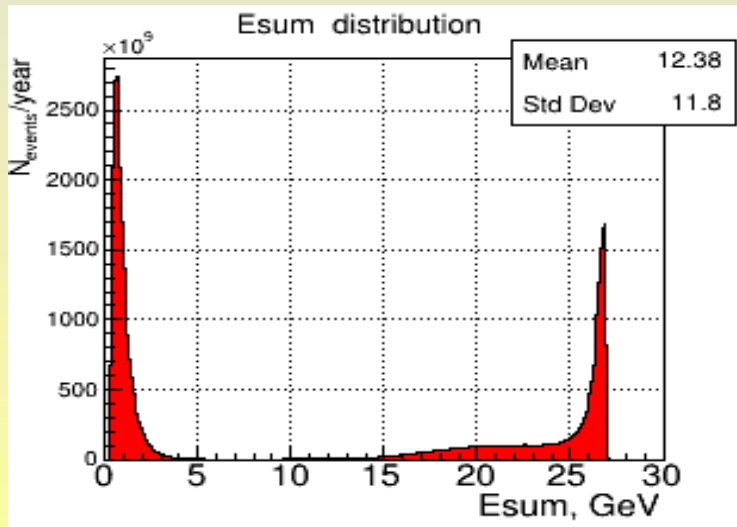
Cut on E_{sum} - summarized energy of all detected particles in event



S
I
G



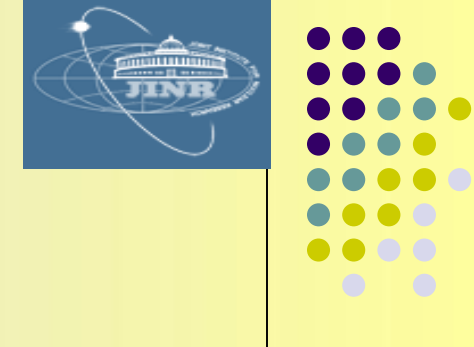
Sig & BKG
in log scale



$E_{\text{sum}} > 26.8 \text{ GeV}$
 $BKG \text{ suppression factor (Eff)} =$
 $58 \text{ (MB)} - 67 \text{ (QCD)}$



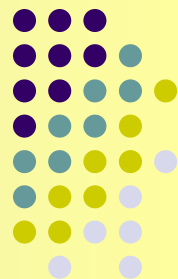
Proposed cuts



1. Events with only **2 muons** with $\text{PT}^\mu > 0.6 \text{ GeV}$, $E^\mu > 1.0 \text{ GeV}$
2. Muons are of the **opposite sign**
3. $M_{\text{inv}}(\mu^+, \mu^-) > 1.0 \text{ GeV}$
4. $\text{PT}_{\text{fast}}^\mu > 1.5 \text{ GeV}$
5. The vertex of production placed within the **distance** from the interaction point $R < 1(30) \text{ mm}$

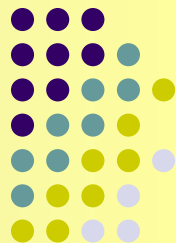
But! Fit program can misidentify μ and π as one track due to small angle of $\pi \rightarrow \mu$ (+ ν) decay .
6. Cut on summarized energy of all detected (without pipe zone and neutrino) particles in event $E_{\text{sum}} > 26.8 \text{ GeV}$
7. Isolation criterion $E_{\text{sum}}^{(\text{R isolation} = 0.2)} < 0.5 \text{ GeV}$

Cuts separate and summarized efficiency for Minimum-bias background events (10^9)



$$\text{Efficiency } \textit{Eff} (K,N) = \text{Nev(cutN)} / \text{Nev(cutK)}$$

N of cuts	S/B ratio	Efficiency for BKG	Rest of BKG	Efficiency for SIG	Rest of SIG
1 <i>Exactly 2μ with $\text{PT}^\mu > 0.6 \text{ GeV}$, $\text{P}(E)^\mu > 1.0 \text{ GeV}$</i>	$5.1 * 10^{-4}$	Eff (1,init) = 3480	$2.9 \times 10^{-2} \%$	2.3	44.1 %
2+1 <i>2μ are of the opposite sign</i>	$8.9 * 10^{-4}$	Eff (2,1) = 1.8	$1.6 \times 10^{-2} \%$	1.01	43.8 %
3+2+1 <i>$M_{inv}(\mu^+, \mu^-) > 1.0 \text{ GeV}$</i>	$1.2 * 10^{-3}$	Eff (3,2) = 1.3	$1.2 \times 10^{-2} \%$	1.01	43.8 %
4+3+2+1 <i>$\text{PT}^\mu_{Emax} > 1.5 \text{ GeV}$</i>	$1.1 * 10^{-2}$	Eff (4,3) = 13.2	$9.1 \times 10^{-4} \%$	1.43	30.5 %
5+3+2+1 <i>$E_{sum}^{all} > 26.8 \text{ GeV}$</i>	$2.6 * 10^{-2}$	Eff (5,3) = 58.3	$2.1 \times 10^{-4} \%$	2.63	16.6 %
6+3+2+1 <i>$\text{PT}_{vecsum}^{all} < 0.2 \text{ GeV}$</i>	$2.9 * 10^{-3}$	Eff (6,3) = 4.1	$2.9 \times 10^{-3} \%$	1.70	25.7 %
7+3+2+1 <i>$P_{vecsum}^{all} < 0.2 \text{ GeV}$</i>	$9.4 * 10^{-3}$	Eff (7,3) = 18.4	$6.5 \times 10^{-4} \%$	2.34	18.7 %
8+3+2+1 <i>Isolation criterium</i>	47.6	Eff (8,3) = 30177	$4.0 \times 10^{-7} \%$	1.01	43.2 %
9+3+2+1 <i>$R_{vertex} < 1 \text{ mm}$</i>	$8.5 * 10^{-1}$	Eff (9,3) = 710	$1.7 \times 10^{-5} \%$	1.01	43.5 %
10+3+2+1 <i>$R_{vertex} < 30 \text{ mm}$</i>	$7.1 * 10^{-1}$	Eff (10,3) = 597	$2.0 \times 10^{-5} \%$	1.01	43.5 %
5+4+3+2+1 <i>$E_{sum}^{all} > 26.8 \text{ GeV}$</i>	$2.3 * 10^{-1}$	Eff (5,4) = 52.7	$1.7 \times 10^{-5} \%$	2.52	12.1 %
8+4+3+2+1 <i>Isolation criterium</i>	24.7	Eff (8,4) = 2280	$4.0 \times 10^{-7} \%$	1.02	29.9 %
8+5+4+3+2+1 <i>Isolation criterium</i>	> 54	Eff (8,5) > 173	< $1.0 \times 10^{-7} \%$	1.87	16.3 %

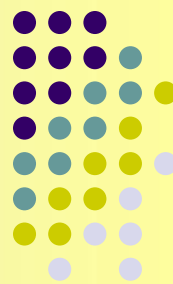


Cuts separate and summarized efficiency for QCD (+charmonia) background events (10^9)

Efficiency Eff (K,N) = Nev(cutN) / Nev(cutK)

N of cuts	S/B ratio	Efficiency for BKG	Rest of BKG	Efficiency for SIG	Rest of SIG
1 <i>Exactly 2μ with $PT^\mu > 0.6$ GeV, $P(E)^\mu > 1.0$ GeV</i>	$4.4 * 10^{-5}$	Eff (1,init) = 2471	$4.0 \times 10^{-2} \%$	2.8	35.3 %
2 ⁺¹ <i>2μ are of the opposite sign</i>	$7.4 * 10^{-5}$	Eff (2,1) = 1.7	$2.3 \times 10^{-2} \%$	1.2	33.3 %
3 ⁺²⁺¹ <i>$M_{inv}(\mu^+, \mu^-) > 1.0$ GeV</i>	$1.0 * 10^{-4}$	Eff (3,2) = 1.3	$1.7 \times 10^{-2} \%$	1.0	33.3 %
4 ⁺³⁺²⁺¹ <i>$PT^\mu_{Emax} > 1.5$ GeV</i>	$7.4 * 10^{-4}$	Eff (4,3) = 14.1	$1.2 \times 10^{-3} \%$	1.9	17.6 %
5 ⁺³⁺²⁺¹ <i>$E_{sum}^{all} > 26.8$ GeV</i>	$2.4 * 10^{-3}$	Eff (5,3) = 67.4	$2.5 \times 10^{-4} \%$	2.8	11.7 %
6 ⁺³⁺²⁺¹ <i>$PT_{vecsum}^{all} < 0.2$ GeV</i>	$2.5 * 10^{-4}$	Eff (6,3) = 4.2	$4.0 \times 10^{-3} \%$	1.7	19.6 %
7 ⁺³⁺²⁺¹ <i>$P_{vecsum}^{all} < 0.2$ GeV</i>	$9.3 * 10^{-4}$	Eff (7,3) = 19.7	$8.6 \times 10^{-4} \%$	2.2	15.7 %
8 ⁺³⁺²⁺¹ <i>Isolation criterium</i>	> 17	Eff (8,3) > 169847	$< 1.0 \times 10^{-7} \%$	1.0	33.3 %
9 ⁺³⁺²⁺¹ <i>$R_{vertex} < 1$ mm</i>	$5.5 * 10^{-2}$	Eff (9,3) = 551	$3.0 \times 10^{-5} \%$	1.0	33.3 %
10 ⁺³⁺²⁺¹ <i>$R_{vertex} < 30$ mm</i>	$4.8 * 10^{-2}$	Eff (10,3) = 479	$3.5 \times 10^{-5} \%$	1.0	33.3 %
5 ⁺⁴⁺³⁺²⁺¹ <i>$E_{sum}^{all} > 26.8$ GeV</i>	$1.6 * 10^{-2}$	Eff (5,4) = 64.5	$1.8 \times 10^{-5} \%$	3.0	5.9 %
8 ⁺⁴⁺³⁺²⁺¹ <i>Isolation criterium</i>	> 9	Eff (8,4) > 12066	$< 1.0 \times 10^{-7} \%$	1.0	17.6 %
8 ⁺⁵⁺⁴⁺³⁺²⁺¹ <i>Isolation criterium</i>	> 3	Eff (8,5) > 187	$< 1.0 \times 10^{-7} \%$	1.0	5.9 %

Conclusion



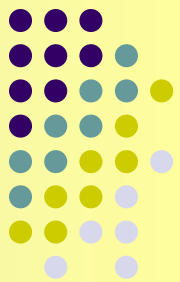
The proposed cuts:

1. Events with only **2** muons with $\text{PT}^\mu > 0.6 \text{ GeV}$, $E^\mu > 1.0 \text{ GeV}$
2. Muons are of the **opposite sign**
3. **$M_{\text{inv}}(\mu^+, \mu^-) > 1.0 \text{ GeV}$**
4. **$\text{PT}^\mu_{\text{fast}} > 1.5 \text{ GeV}$**
5. Cut on summarized energy of all detected (without pipe zone and neutrino) particles in event $E_{\text{sum}} > 26.8 \text{ GeV}$
6. Isolation criterion $E_{\text{sum}}^{\text{isolation}} (\text{R isolation} = 0.2) < 0.5 \text{ GeV}$

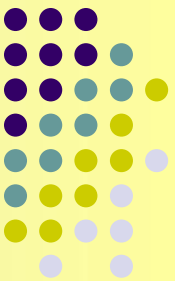
*Allow (in the ideal case) to suppress Mini-bias bkgd up to **S/B ~ 50**,
QCD background – up to **S/B >~ 17**.*

The SPD Collaboration made a decision to suspend the study of such reactions.

In fact, taking into account the detector and additional contributions of muon misidentification,
it will be difficult to experimentally isolate the DY signal from the combinatorial background.

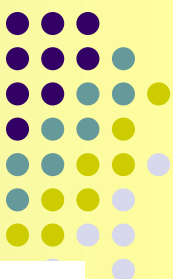


Thank you for your attention!

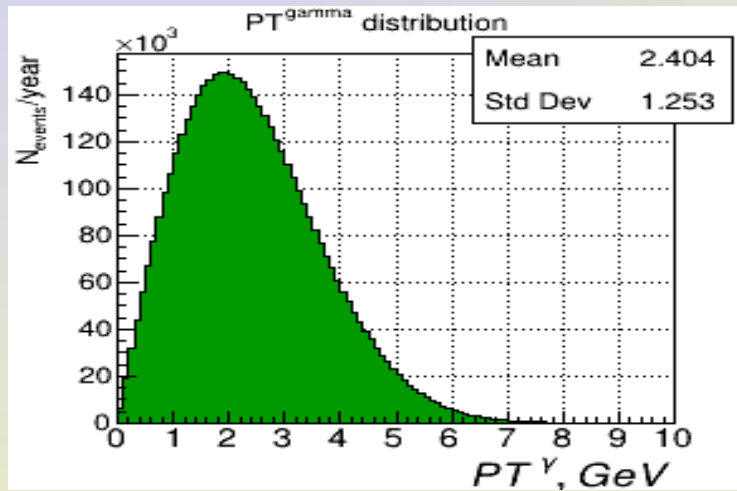


Back up slides

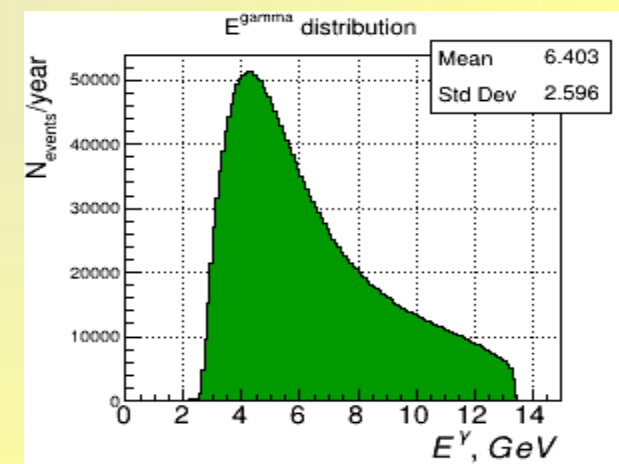
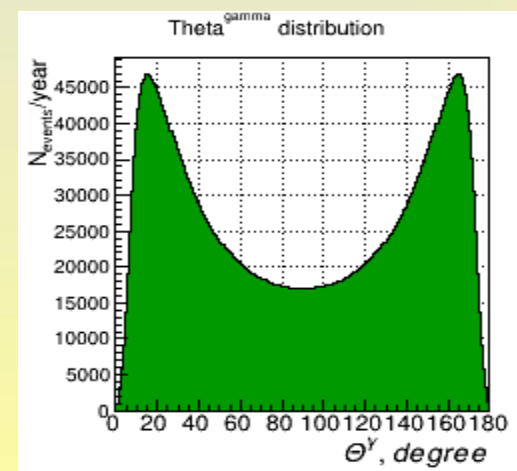
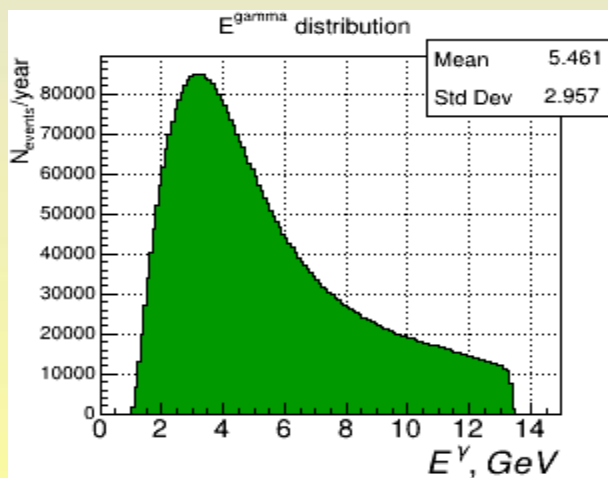
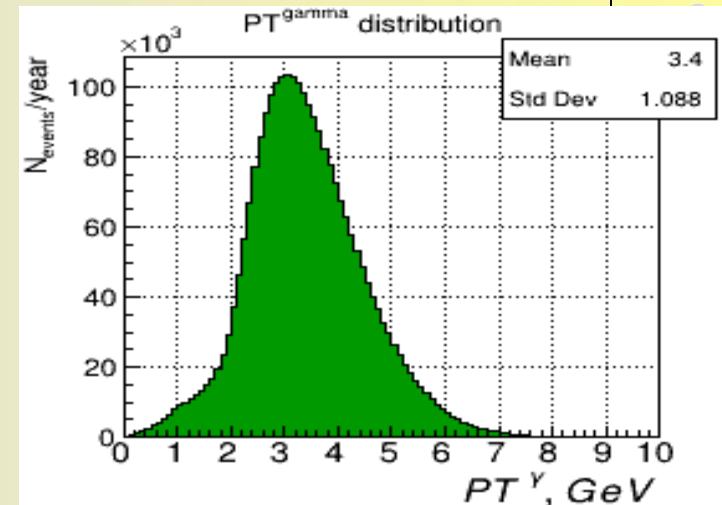
Intermediate γ^* distributions



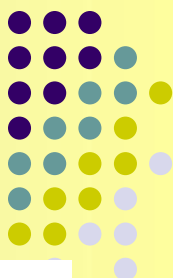
Without cuts



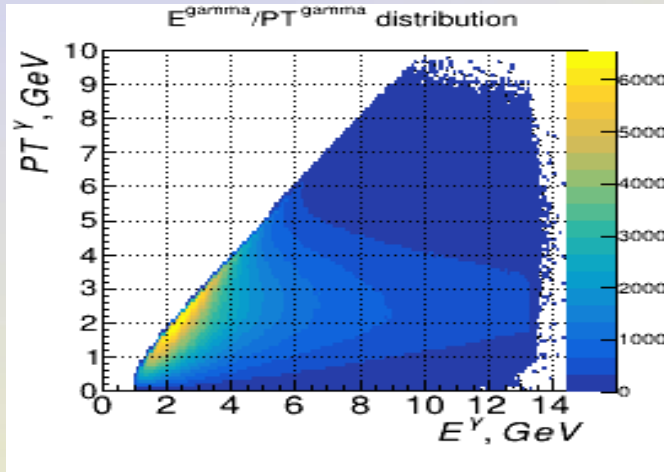
After cuts



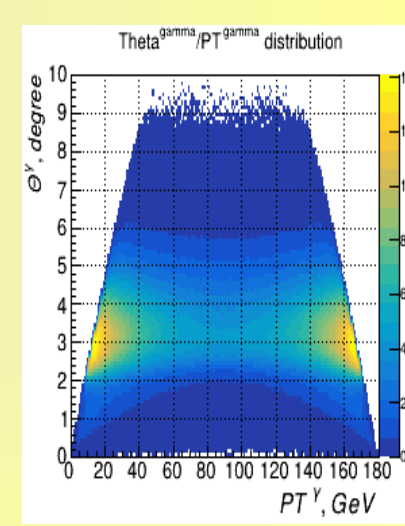
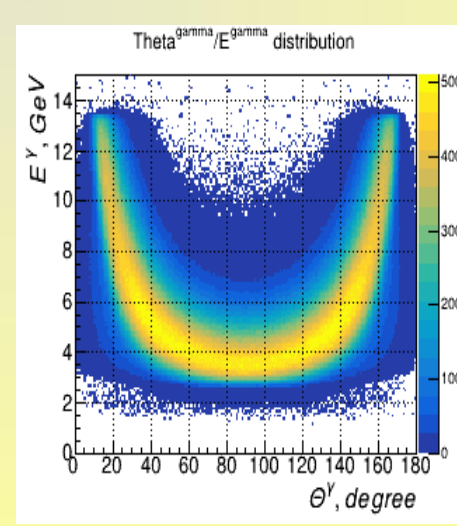
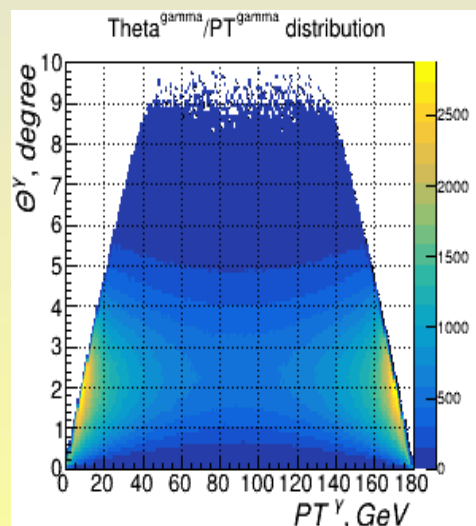
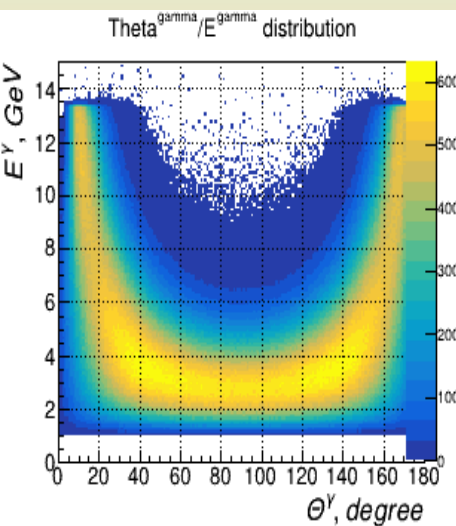
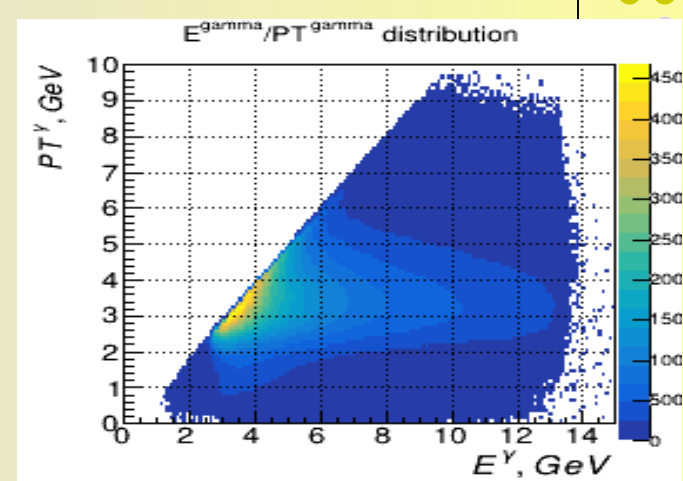
Intermediate γ^* correlation distributions



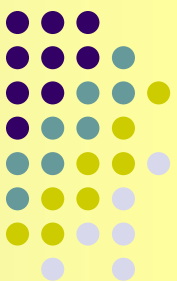
Without cuts



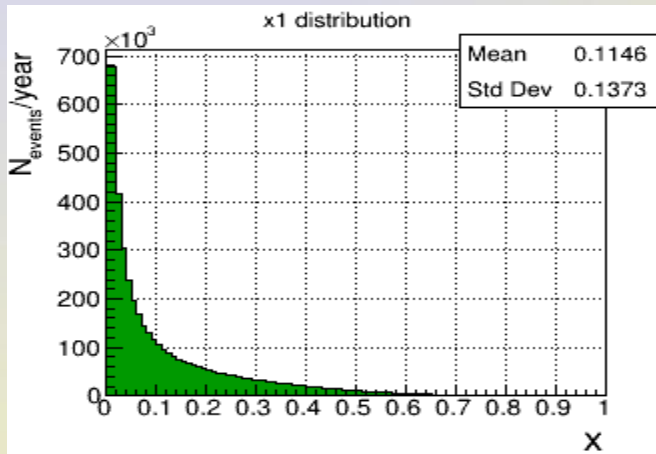
After cuts



General Drell-Yan event variables for pp collision at $E = 27 \text{ GeV}$

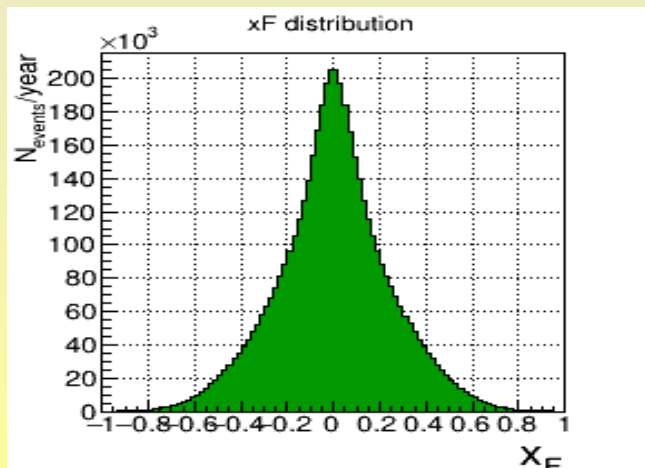


Доля импульса x , уносимая партонами

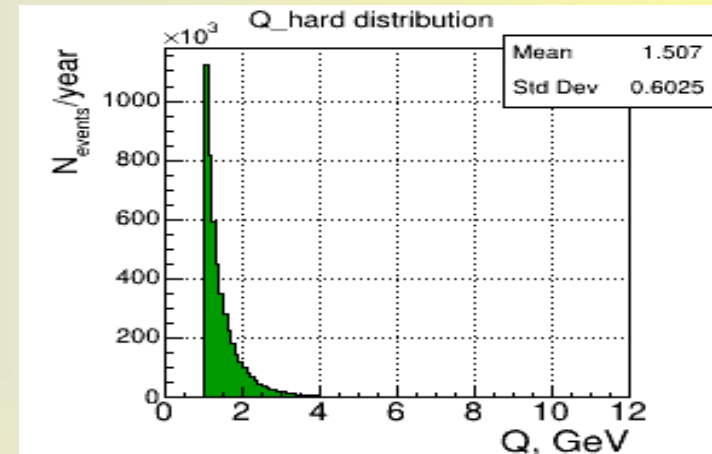


$$X = X_1 - X_2$$

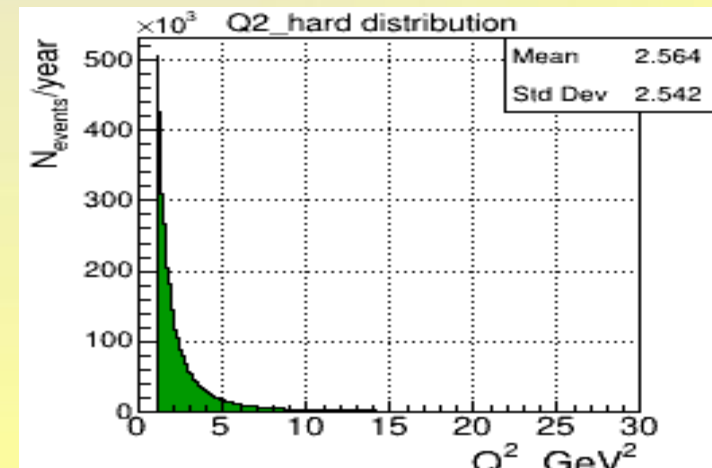
$$F = 1 - 2$$



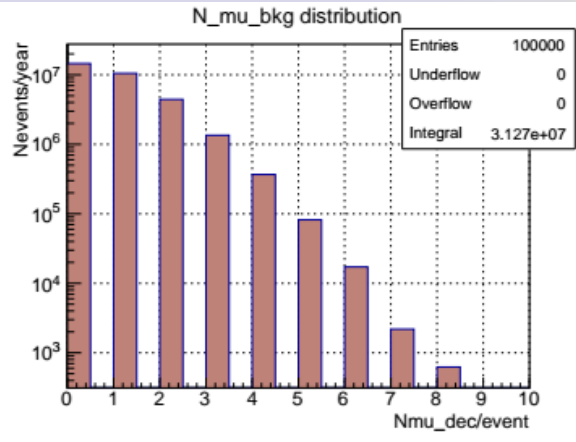
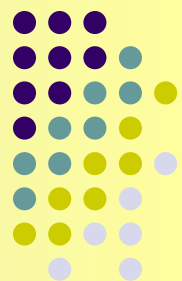
cms
Q жесткого подпроцесса



$$Q^2 \text{ жесткого подпроцесса}$$

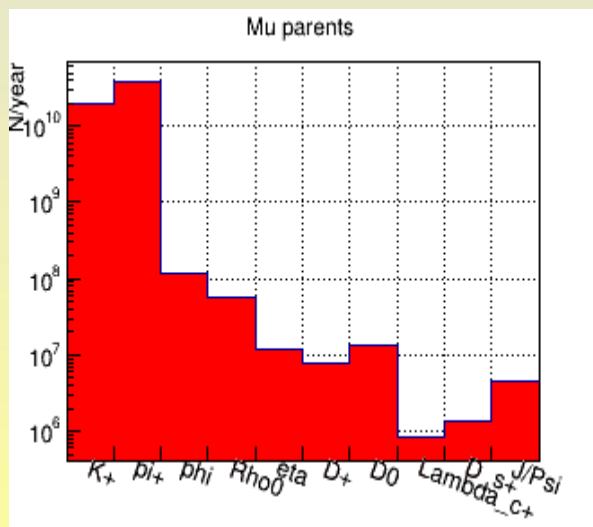


Background muons in signal events



53.5 % of signal events contains >2 muons
 - up to 8 μ /event

We allow particles decay (and produce muons) in the volume before Muon (Range) System :
 cylindr radius **R = 2 400 mm**,
 size from the centre along Z axis **L = 4 000 mm**
 and search for muons in the angle region **9° < Θ < 171°**

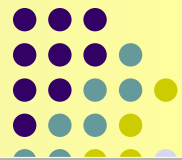


The most probable parents of bkg muons - are charged π and K

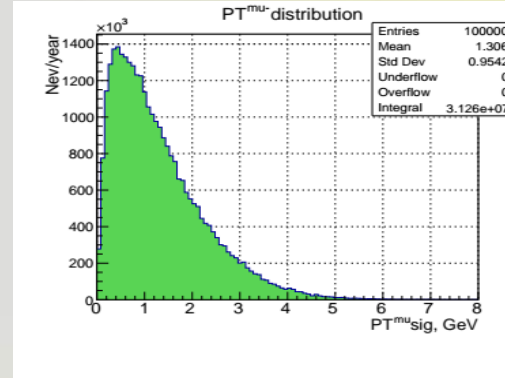
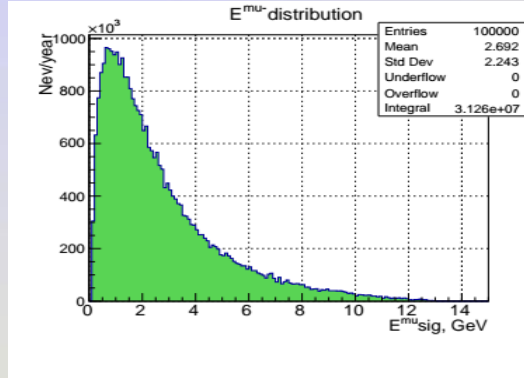
*The most probable grandparents of bkg muons
 - are «string» (Lund model),*

$$\rho^0, \rho^+, K^0, K^+, K^*, K^0, \eta'$$

Decay muons in signal events



S
I
G



Cuts :
exactly
2 muons

$E > 0.8$
GeV
 $PT > 0.4$
GeV

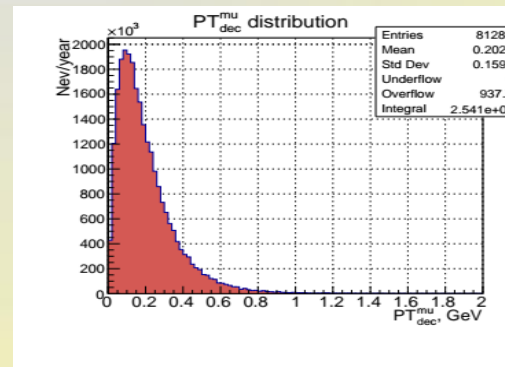
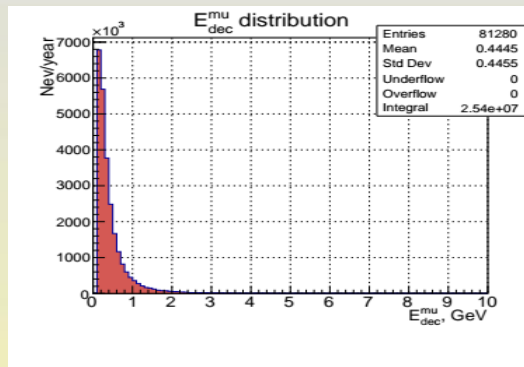
$E > 1.0$
GeV
 $PT > 1.0$
GeV

Reminder
of signal
events

54.1%

23.5%

D
E
C

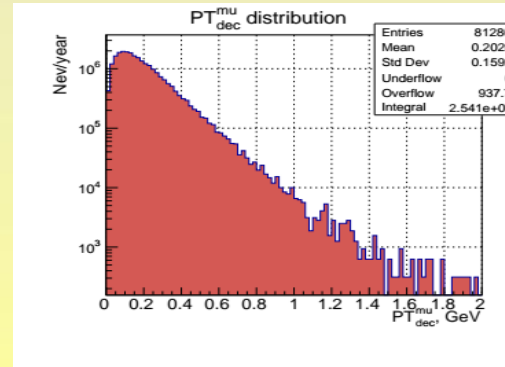
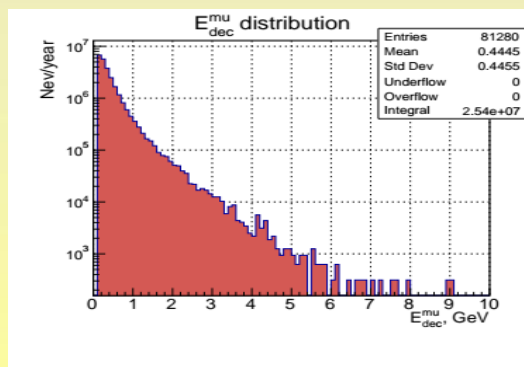


Fraction
of initial
signal
events
with
additional
muons

2.1%

0.08%

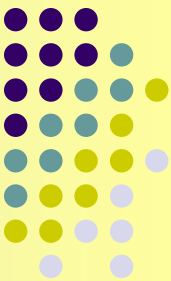
D
E
C
(log)



Fraction
of
remaining
signal
events
with
additional
muons

3.9 %

0.3%



Another situation when we have exactly 2 μ — first signal, the second — survived fake one.

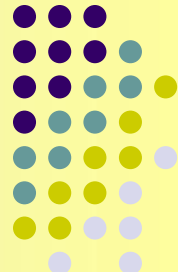
We have 2 situations -

1. Muons are of the same sign — easy to cut off
2. Muons are of different signs

After cutting off the events with additional (>2) muons we have

Cuts: exactly 2 muons with opposite signs	$E > 0.8 \text{ GeV}$ $\text{PT} > 0.4 \text{ GeV}$	$E > 1.0 \text{ GeV}$ $\text{PT} > 1.0 \text{ GeV}$
Reminder of signal events	51.9%	23.4%
Fraction of initial signal events with fake muons of the same sign	0.9%	0.09%
Fraction of remaining signal events with muons of the same sign	1.7 %	0.4%
Reminder of signal events after cut off the events with the muons of the same sign	51.0%	23.4%
Fraction of initial signal events with fake muons of different sign	0.9%	0.1%
Fraction of remaining signal events with muons of different sign	1.8 %	0.4%

Processes with charmonium production



86) $g g \rightarrow J/\Psi + g \rightarrow l^+l^- + X$

R.Baier and R.Rücke, Z.Phys. C19 (1983) 251

106) $g g \rightarrow J/\Psi + \gamma \rightarrow l^+l^- + X$

M.Drees and C.S.Kim, Z.Phys. C53 (1991) 673

421) $g g \rightarrow c\bar{c}^- [{}^3S_1 {}^{(1)}] g \rightarrow ll + X$

431) $g g \rightarrow c\bar{c}^- [{}^3P_0 {}^{(1)}] g \rightarrow ll + X$

422) $g g \rightarrow c\bar{c}^- [{}^3S_1 {}^{(8)}] g \rightarrow ll + X$

432) $g g \rightarrow c\bar{c}^- [{}^3P_1 {}^{(1)}] g \rightarrow ll + X$

423) $g g \rightarrow c\bar{c}^- [{}^3S_0 {}^{(8)}] g \rightarrow ll + X$

433) $g g \rightarrow c\bar{c}^- [{}^3P_2 {}^{(1)}] g \rightarrow ll + X$

424) $g g \rightarrow c\bar{c}^- [{}^3P_J {}^{(8)}] g \rightarrow ll + X$

434) $g q \rightarrow c\bar{c}^- [{}^3P_0 {}^{(1)}] q \rightarrow ll + X$

425) $g q \rightarrow c\bar{c}^- [{}^3S_1 {}^{(8)}] q \rightarrow ll + X$

435) $g q \rightarrow c\bar{c}^- [{}^3P_1 {}^{(1)}] q \rightarrow ll + X$

426) $g q \rightarrow c\bar{c}^- [{}^3P_J {}^{(8)}] q \rightarrow ll + X$

436) $g q \rightarrow c\bar{c}^- [{}^3P_2 {}^{(1)}] q \rightarrow ll + X$

427) $g g \rightarrow c\bar{c}^- [{}^3S_1 {}^{(1)}] q \rightarrow ll + X$

437) $q q^- \rightarrow c\bar{c}^- [{}^3P_0 {}^{(1)}] g \rightarrow ll + X$

428) $\underline{q q^- \rightarrow c\bar{c}^- [{}^3S_1 {}^{(8)}] g \rightarrow ll + X}$

438) $q q^- \rightarrow c\bar{c}^- [{}^3P_1 {}^{(1)}] g \rightarrow ll + X$

429) $\underline{q q^- \rightarrow c\bar{c}^- [{}^1S_0 {}^{(8)}] g \rightarrow ll + X}$

439) $q q^- \rightarrow c\bar{c}^- [{}^3P_2 {}^{(1)}] g \rightarrow ll + X$

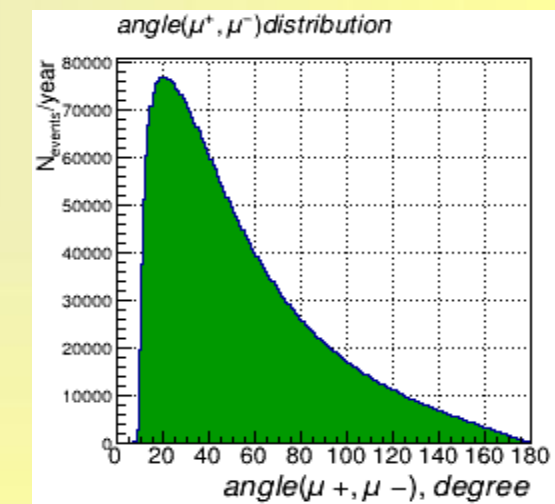
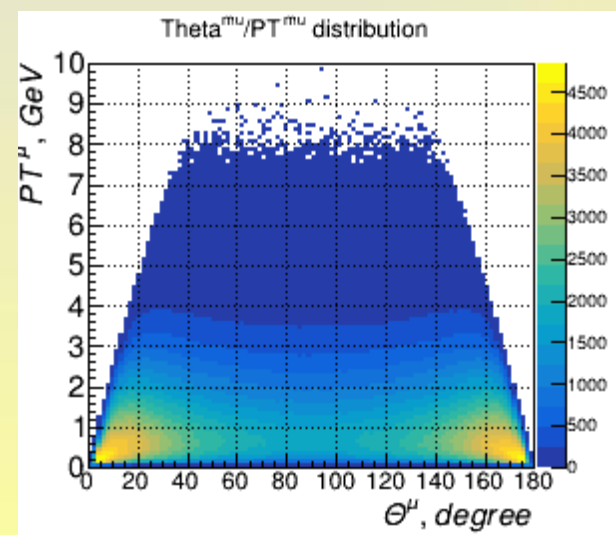
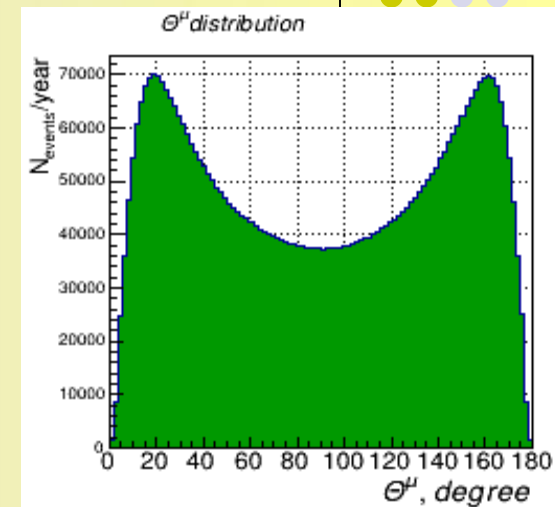
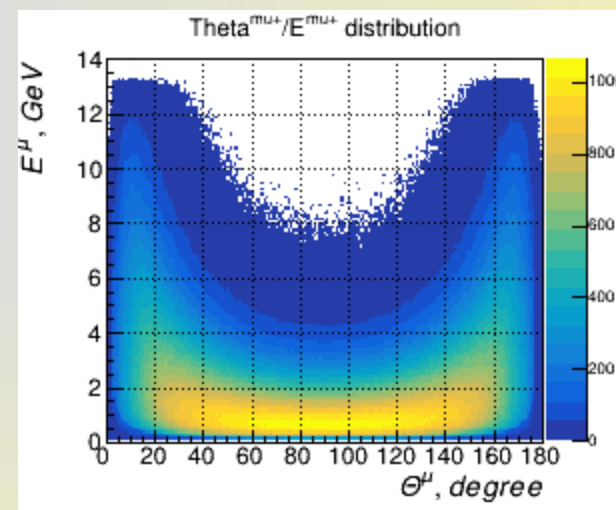
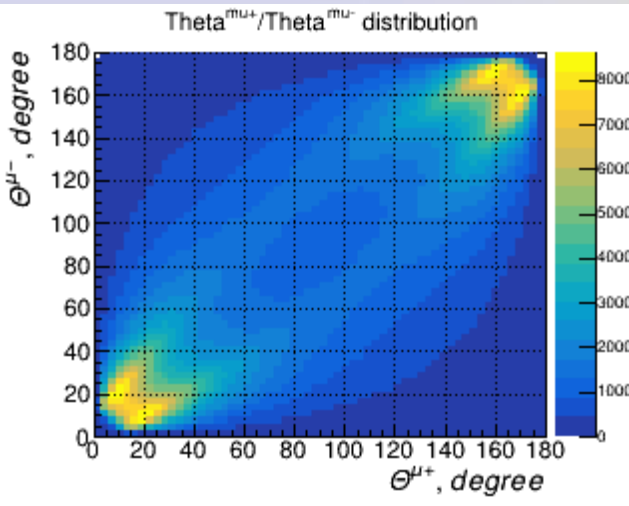
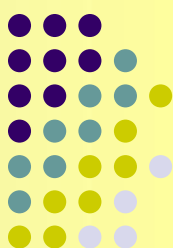
430) $\underline{q q^- \rightarrow c\bar{c}^- [{}^3P_J {}^{(8)}] g \rightarrow ll + X}$

G.T.Badwin, E.Breten and G.P.Lepage, Phys.Rev. D51 (1995) 1125 [Erratum: ibid D55 (1997) 5883];

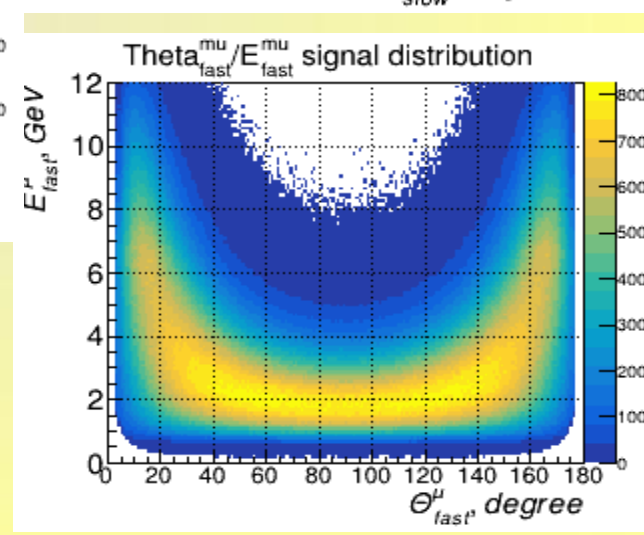
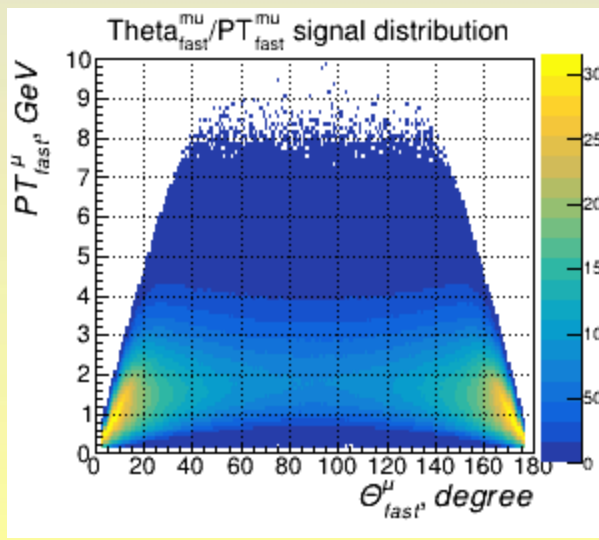
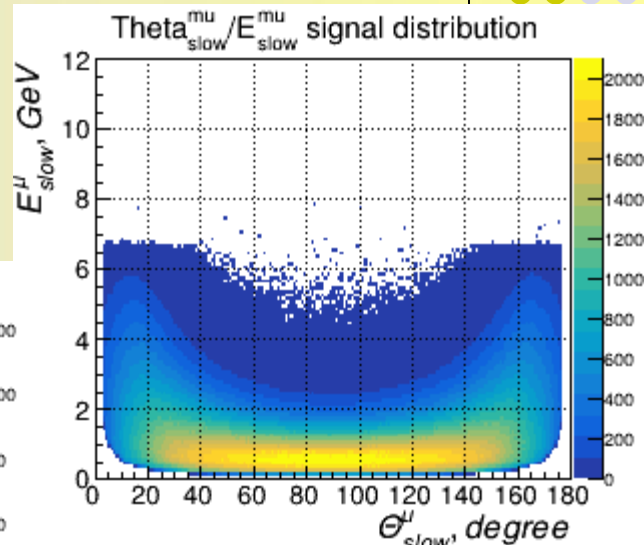
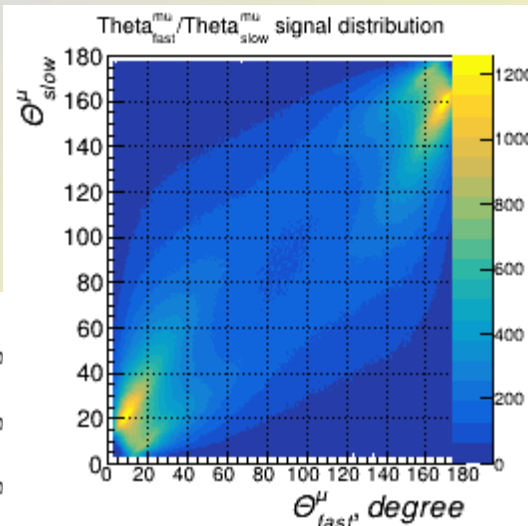
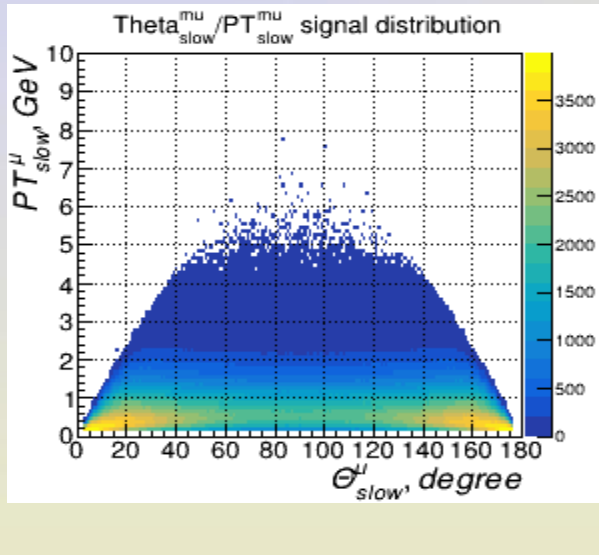
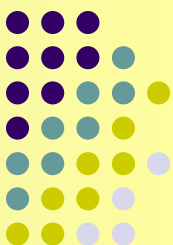
M.Beneke, MKrämer and M.Vänttinen,
Phys.Rev.D57 (1998) 4258;

B.A.Kniehl and J.Lee, Phys.Rev. D62 (2000) 114027

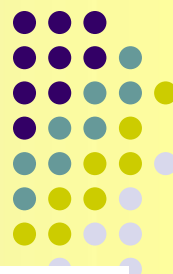
Some signal μ correlation distributions



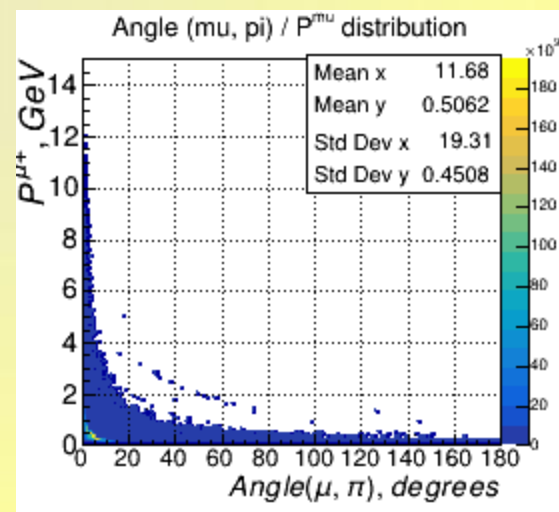
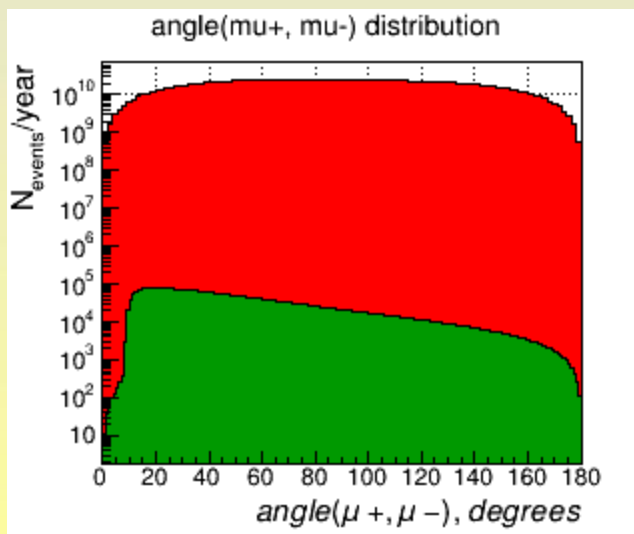
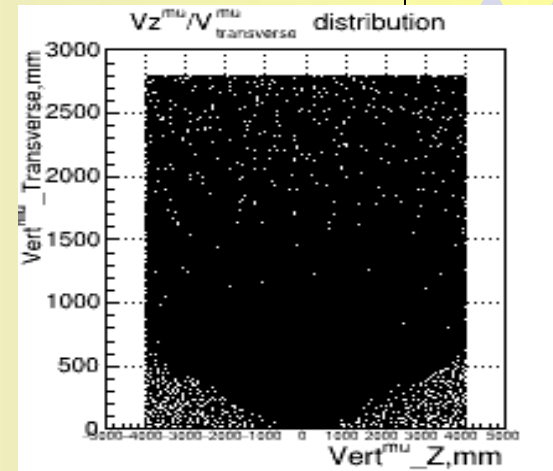
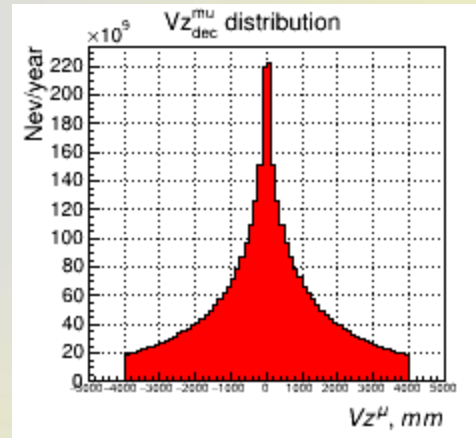
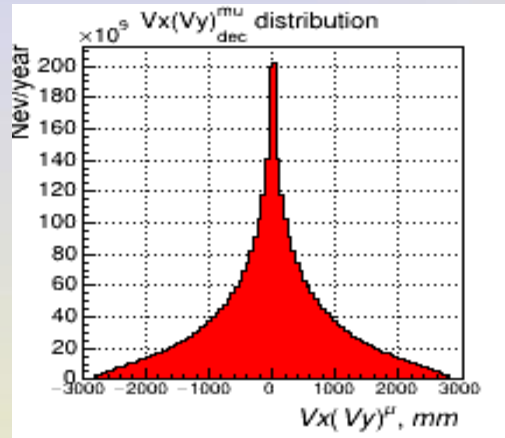
Angle and E, PT for fast and slow signal μ correlation distributions



Vertex & angle distributions

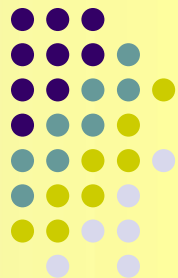


P
Y
T
H
I
A





π/μ rejection



For 5λ of path length in iron.

Particle momentum	π/μ rejection	
0.5 — 1 GeV	~ 80 % (experiment with MS prototype)	EPJ Web Conf., 177 (2018) 04001
1 — 1.5 GeV	~ 90 % (assumption)	
> 1.5 GeV	~ 99 % (assumption)	

The path length of a charged particle track inside the sandwich structure serves as one of the most powerful variables for μ/π separation, which is challenging due to the similar rest mass of muon and pion

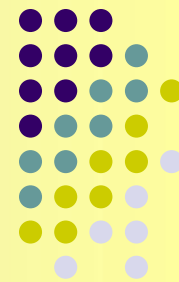
for 3λ path length (+4.9 % muon misidentification)

for 4λ path length (+1.8 % muon misidentification)

for 5λ path length (+0.67 % muon misidentification)

$$\lambda_{FE} \approx 17\text{cm}$$

Cuts separate and summarized efficiency for Open Charm background events (10^7)



Efficiency Eff (K,N) = Nev(cutN) / Nev(cutK)

N of cuts	S/B ratio	Efficiency for BKG	Rest of BKG	Efficiency for SIG	Rest of SIG
1 <i>Exactly 2μ with $PT^\mu > 0.6 \text{ GeV}$, $P(E)^\mu > 1.0 \text{ GeV}$</i>	0.10	Eff (1,init) = 47.14	2.1 %	2.45	40.8 %
2 ⁺¹ <i>2μ are of the opposite sign</i>	0.12	Eff (2,1) = 1.21	1.7 %	1.01	40.5 %
3 ⁺²⁺¹ <i>$M_{inv}(\mu^+, \mu^-) > 1.0 \text{ GeV}$</i>	0.14	Eff (3,2) = 1.19	1.4 %	1.01	40.0 %
4 ⁺³⁺²⁺¹ <i>$PT^\mu_{Emax} > 1.5 \text{ GeV}$</i>	0.82	Eff (4,3) = 8.77	$1.7 \times 10^{-1} \%$	1.53	26.2 %
5 ⁺³⁺²⁺¹ <i>$E_{sum}^{all} > 26.8 \text{ GeV}$</i>	263.3	Eff (5,3) = 5401	$2.7 \times 10^{-4} \%$	2.93	13.6 %
6 ⁺³⁺²⁺¹ <i>$PT_{vecsum}^{all} < 0.2 \text{ GeV}$</i>	1.18	Eff (6,3) = 14.31	$1.0 \times 10^{-1} \%$	1.73	23.1 %
7 ⁺³⁺²⁺¹ <i>$P_{vecsum}^{all} < 0.2 \text{ GeV}$</i>	7.04	Eff (7,3) = 131.6	$1.1 \times 10^{-2} \%$	2.67	15.0 %
8 ⁺³⁺²⁺¹ <i>Isolation criterium</i>	> 20433	Eff (8,3) > 145845	$< 1.0 \times 10^{-5} \%$	1.02	39.3 %
9 ⁺³⁺²⁺¹ <i>$R_{vertex} < 1 \text{ mm}$</i>	764.8	Eff (9,3) = 5401	$2.7 \times 10^{-4} \%$	1.01	39.7 %
10 ⁺³⁺²⁺¹ <i>$R_{vertex} < 30 \text{ mm}$</i>	18.6	Eff (10,3) = 131.6	$1.1 \times 10^{-2} \%$	1.01	39.7 %
5 ⁺⁴⁺³⁺²⁺¹ <i>$E_{sum}^{all} > 26.8 \text{ GeV}$</i>	1306	Eff (5,4) = 4157	$4.0 \times 10^{-5} \%$	2.61	10.0 %
8 ⁺⁴⁺³⁺²⁺¹ <i>Isolation criterium</i>	> 13238	Eff (8,4) > 16627	$< 1.0 \times 10^{-5} \%$	1.03	25.4 %
8 ⁺⁵⁺⁴⁺³⁺²⁺¹ <i>Isolation criterium</i>	> 5178	Eff (8,5) > 4	$< 1.0 \times 10^{-5} \%$	1.01	9.95 %